

## Preparation of Super-hydrophobic Surface on Stainless Steel- A Review

Shah Tanvir Alam Rimon, Fatema Tuz Zohra and Bahram Asiabanpour



Received: 25 March 2025

Accepted: 26 April 2025

Published: 31 July 2025

Publisher: Deer Hill Publications

© 2025 The Author(s)

Creative Commons: CC BY 4.0

### ABSTRACT

This paper presents a thorough examination of the various methodologies employed in the fabrication of superhydrophobic surfaces on stainless steel substrates. The study investigates the chemical, mechanical, and combined processes utilized for surface modification especially for Stainless Steel (SS). Chemical techniques, including etching, sol-gel deposition, coating, and electrochemical deposition methods, are discussed in detail, highlighting their effectiveness in exposing superhydrophobicity to stainless steel surfaces. Mechanical approaches such as laser ablation, micro/nano structuring, and sandblasting are explored, emphasizing their ability to create hierarchical surface roughness conducive to superhydrophobic behaviour. Finally, approaches that combines chemical and mechanical processes to achieve the desirable surface modification are discussed under the combined approach section. This study is helpful to identify which fabrication method would be best suitable for a particular need within available resources. This review provides a comprehensive overview of the state-of-the-art techniques for preparing superhydrophobic surfaces on stainless steel, offering insights into the advancements, challenges, and future directions in this area of research.

**Keywords:** Surface wettability, Stainless steel, Superhydrophobicity, Surface modification.

### 1 INTRODUCTION

#### 1.1 Hydrophobicity

Nature generously fascinates us with its various sources and features. Not only that, but it also has various effects on our daily lives through the manifestation of its mysterious characteristic behaviour. Nature is the primary stimulus for researchers to explore new horizons. Superhydrophobicity is one such property found in nature that leads us to open new technological horizons. The super-hydrophobicity was initially noted on lotus leaves and other plant leaves that refused to become wet in the natural world. Because the surface's micro and nanoscopic architecture lowers the droplet's adherence to it, water droplets pick up dirt. Other plants, including *Tropaeolum* (nasturtium), *Opuntia* (prickly pear), *Alchemilla*, cane, and some insect's wings, also possess super-hydrophobicity and self-cleaning qualities [1]. The lotus effect is a term used to describe the self-cleaning qualities of super-hydrophobicity, as seen in lotus flowers with microstructures [2]. Surfaces that repel water are classified as hydrophobic or super-hydrophobic. An apparent contact angle of more than 150 degrees and a sliding angle of fewer than 10 degrees describe a superhydrophobic surface. Superhydrophobic interaction repels water, so droplets do not flatten but roll off. Super-hydrophobic surfaces are exceptionally difficult to wet due to their extraordinary hydrophobicity. To be more precise, super-hydrophobic refers to a higher degree of hydrophobicity [3]. Over the past two decades, the scientific community has paid close attention to superhydrophobic surfaces due to their potential for practical applications and special water-repellent, self-cleaning capabilities [4]–[10].

#### 1.2 Stainless Steel and Hydrophobicity

Stainless steel is used in every sector, including medical technology, building trade, aircraft construction, food and catering, automobile, and marine industries [11]–[14]. The use of stainless steel in power plants helps them avoid meltdowns. Because stainless steel is used in piping systems, it is possible to provide water without risk of contamination [15]. Stainless steel is used in every industry that can be thought of. That is why stainless steel is selected despite the many metals available. Despite having inherent corrosion resistance, stainless steel rusts in specific

---

Shah Tanvir Alam Rimon<sup>1</sup>, Fatema Tuz Zohra<sup>2</sup> ✉, Bahram Asiabanpour<sup>2</sup>

<sup>1</sup>Department of Mechanical Engineering, Rajshahi University of Engineering & Technology (RUET), Station Rd, Rajshahi 6204, Bangladesh

<sup>2</sup>Materials Science, Engineering, and Commercialization, Texas State University, 601 University Dr, San Marcos, TX 78666, USA

E-mail: fatema\_zohra@txstate.edu

Reference: Rimon, S.T.A., Zohra, F. and Asiabanpour, B. (2025). Preparation of Super-hydrophobic Surface on Stainless Steel: A Review. International Journal of Engineering Materials and Manufacture, 10(3), 44-70.

environments, but not as quickly as ordinary steel. Stainless steel corrodes over time when it is exposed to heat, salt, or dangerous chemicals [16]. This stainless-steel damage or corrosion may result in significant direct and indirect losses in many industries. It may occasionally bring about a severe catastrophe in daily life, as listed in **Table 1**. Because of these consequences, stainless steel preservation is essential. The super-hydrophobicity of stainless steel makes it highly anti-corrosive, ultraviolet (UV) resistant, mechanically more durable, and more stable in corrosive medium, as reported in numerous articles [7], [9], [17]–[24]. Super-hydrophobic coatings are widely applied for self-cleaning, anti-corrosion, oil-water separation, anti-icing, anti-fouling, anti-scaling, anti-fogging and numerous medical purposes [25].

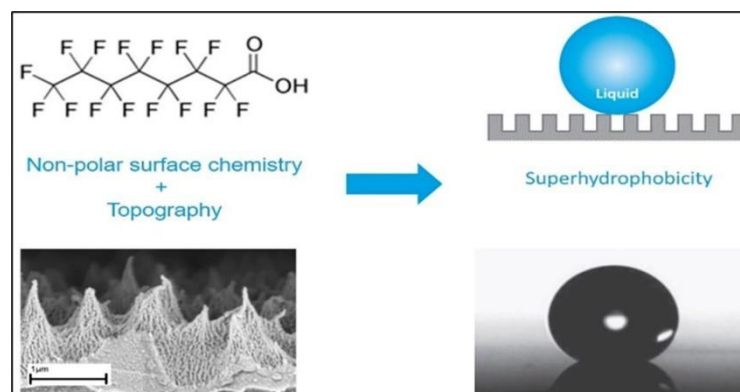
**Table 1:** List of some renowned accidents due to stainless steel corrosion [26].

	Incident	Reason	Damages
1	Bhopal Accident, 1984, Bhopal	Corrosion in valves, pipelines, and other safety devices.	Methylisocyanate (MIC) storage tank leakage.
2	Swimming Pool Roof, 1985, Switzerland	Stress corrosion	Roof collapse and twelve deaths.
3	Guadalajara Sewer Explosion, 1992, Mexico	Rusting of pipeline obstructed by gasoline.	1600 building damage, 215 deaths, and 1500 injuries.
4	Carlsbad Pipeline explosion, 2000, New Mexico, USA	Corrosion in gas pipeline	Natural Gas explosion

Superhydrophobic surfaces have a drag reduction ratio of about 40–50% compared to untreated surfaces at moderate speeds [27]. Superhydrophobic stainless steel was fabricated by combining laser patterning and nano polytetrafluoroethylene (PTFE) sputtering, which improved the wettability behaviour and made the material appropriate for the hemocompatibility of blood contact devices [28]. However, slippery liquid-infused surfaces fabricated on stainless steel via femtosecond laser ablation, followed by fluorosilanization, revealed outstanding fouling-release performances [29]. Moreover, super-hydrophobicity can provide more corrosion resistance properties on stainless steel, making the SS more feasible in the food and dairy industry [30], [31]. Porous stainless steel fabricated by selective laser sintering (SLS) and traditional sintering has significant applications in the medical sector [32]. Bacterial and cell adherence can be inhibited and prevented on medical equipment surfaces using a superhydrophobic surface (SHS) [33]. In the Navy, ice cover has long been a problem. Super-hydrophobic surfaces can improve a ship's ability to resist ice, which is crucial for ships operating in cold, low-latitude environments [34]–[40].

### 1.3 Fabrication of Superhydrophobic Stainless Steel

Super-hydrophobicity depends on two characteristics: non-wetting chemistry and micro or nanostructured topography. **Figure 1** illustrates that roughness is also necessary for super-hydrophobic surfaces because surface chemistry alone cannot produce them [41].



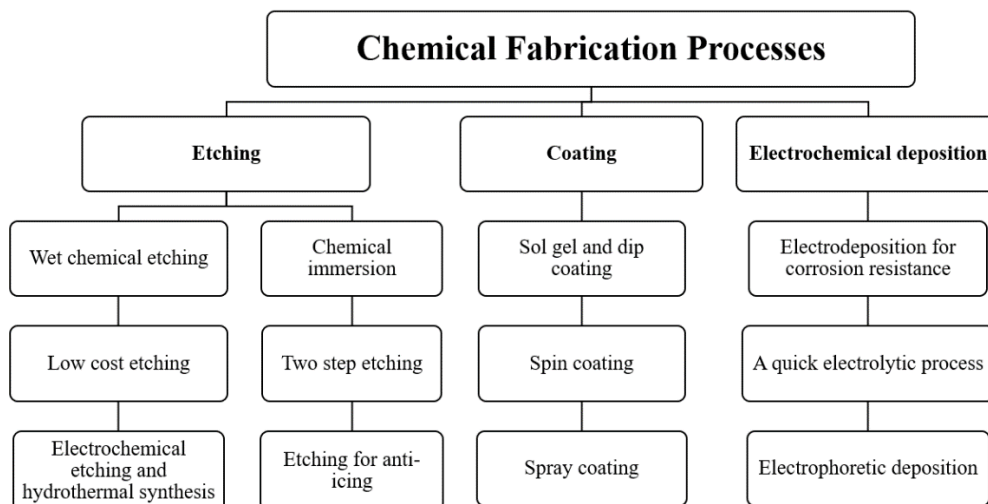
**Figure 1:** Non-wetting chemistry and surface roughness for Super-hydrophobicity [41].

The fabrication process of SHS on materials is performed in two basic steps. First creating surface roughness and second, modifying that rough surface using low surface energy materials to achieve desired results. A low-cost, less time-consuming one-stage chemical etching and assembly process was implemented for obtaining super-hydrophobicity. When exposed to air, the prepared surface showed 16 times better corrosion resistance than the untreated sample and retained its superhydrophobicity for up to 60 days [17]. However, researchers proposed a highly effective and low-cost biomimetic super-hydrophobic surface fabrication process, but this method could not confer an exclusive anti-frosting property [42]. Coating is another superhydrophobic surface fabrication process that successfully fabricated an SHS surface with high resistance to acid and alkali solutions [43]. Layer by layer is an excellent fabrication method that could fabricate a highly UV-resistant super-hydrophobic surface. However, the as-prepared surface was not much durable in a highly acidic solution [44]. It was possible to create super-hydrophobic

stainless steel with good stability in strongly acidic and alkaline solutions using the typical fabrication technique of electrochemical deposition. Additionally, the prepared surface maintained its stability in ambient conditions for 413 days [45]. Some process developed SHS SS surface with anti-biofouling property [46], and many processes could make highly mechanically stable surface [47]. Laser processing was also used to attain self-cleaning, more durable SHS on SS [48], [49]. Although some researchers used some mechanical procedures, it was clear from most of the literature that they concentrated on chemical processes for creating super-hydrophobic surfaces on SS. However, fabrication technologies are desired to be strong, durable, affordable, rapid, and environmentally friendly. Because of this, the fabrication procedure for stainless steel super-hydrophobic surface is given priority in this literature. A series of techniques were explored by numerous researchers to achieve super-hydrophobicity on stainless steel—chemical etching, coating, electrochemical deposition, laser texturing, thermal spraying, and many more. Some of these procedures utilized chemical substrates or solutions for super-hydrophobicity generation, and others used machinery. This review categorizes all the processes into three main categories: chemical, mechanical, and combined approach. Thus, it would be easier to choose an economical, quick, and environmentally friendly fabrication technique.

## 2 CHEMICAL PROCESS OF FABRICATION

A chemical process involves a chemical reaction that can happen naturally or be triggered by an external factor. In other words, a chemical process involves one or more modifications to a substance's chemical composition, physical characteristics, or chemical qualities [50]. For many industrial areas, transforming a material surface into a superhydrophobic one may be essential for several purposes. Currently, several chemical methods are primarily utilized to make the surface of stainless steel superhydrophobic, as shown in **Figure 2**. Current research has developed many chemical fabrication methods for SHS based on etching [51]–[57], coating [58]–[65], electro-deposition [45], [66]–[69], and so on.



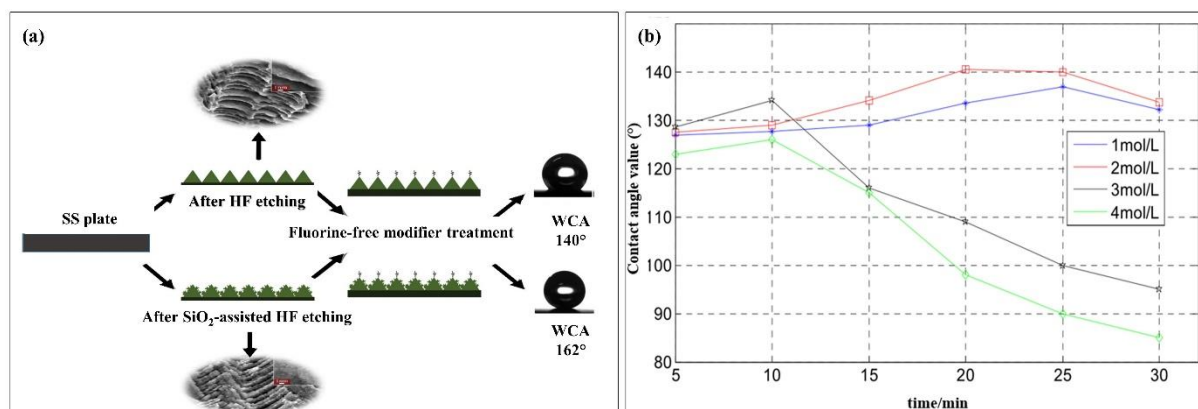
**Figure 2:** Overview of the fabrication methods used to transform stainless steel surfaces to super hydrophobic.

### 2.1 Etching

Etching is a procedure that allows superhydrophobic coatings to be created on surfaces without the use of sophisticated equipment, expensive materials, or complicated steps [70]. Etching is a low-cost, straightforward method commonly used to create heterogeneous surfaces with high roughness [71]. Acid and base etching [72], [73], metal-assisted chemical etching [74], electrochemical etching [75], and other etching procedures can be categorized based on the composition of the metal. **Figure 3** (a) represents a SiO<sub>2</sub>-assisted HF etching for fabricating super-hydrophobicity on stainless steel surfaces [76].

#### 2.1.1 Wet Chemical Etching

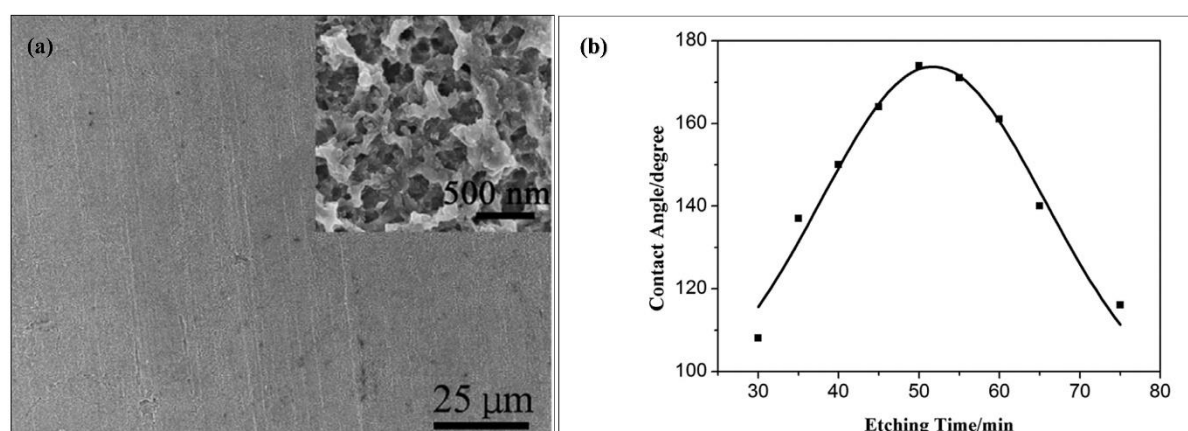
For many industrial applications where stainless steel-fluid contact occurs, including the petrochemical, power generating, maritime, culinary, and construction industries, the wettability qualities of stainless steel (SS) are of significant interest. A simple wet chemical etching process was proposed to establish an SHS on SS plates that would be convenient and inexpensive compared to the traditional methods, and it was carried out in two steps: chemical etching and surface fluorination [77]. Steel plates were polished and cleaned. Different concentrations of hydrochloric acid (HCl) and hydrogen peroxide (H<sub>2</sub>O<sub>2</sub>) mixed solutions was used as etching solution for creating micro-nano structures, and solution of 1H,1H,2H,2H-Perfluorooctyltriethoxysilane (FOTS) used for fluorination purpose. Etching duration and etching solution concentration were also investigated, and according to **Figure 3** (b) [77], it was found that a concentration of HCl 2mol/L and an etching time of 20 minutes were optimal conditions, resulting in a maximum water contact angle (WCA) of 152°.



**Figure 3:** (a) Fabrication process of superhydrophobic surface on stainless steel by SiO<sub>2</sub>-assisted HF etching [76], (b) The relationship between contact angles and concentrations [77].

### 2.1.2 One Step Etching

With anti-corrosion treatments, stainless steel typically has a longer lifespan and requires less maintenance [78]. A low-cost, less time-consuming one-stage chemical etching and assembly process was used [17] to obtain the anti-corrosion performance of a super-hydrophobic surface on SUS 304 stainless steel. Using HCl as the etching solution and FTOS solution for utilizing film on SS was a low-cost procedure. At the same time, instead of using a high-temperature casting technique or an electrodeposition approach, the fabrication procedure may be carried out at room temperature [79], [80]. The one-stage procedure described in [17] combined chemical etching and low surface-energy materials assembling. Both the etching and assembly processes were completed simultaneously. The stainless-steel substrate was etched in HCl solution (1 M), and then FTOS films were created. It was revealed that the longer etching decreases contact angle, and the HCl concentration also affects the hydrophobicity. A “honeycomb” 3D network structure ((Figure 4 (a)) was developed at 50 min etching time. However, the optical condition for obtaining the highest WCA was 1 M concentration of HCl and 50 min etching time (Figure 4 (b)) at 35 °C [17].



**Figure 4:** (a) The “honeycomb” 3D network structure, (b) The relation between contact angle and etching time [17].

The unique one-step chemical approach was employed [81] to modify the surface of 316 SLS to increase hydrophobicity. To induce super-hydrophobicity on stainless steel, H<sub>2</sub>O<sub>2</sub>, HF, and perfluorooctyl trichlorosilane (PFOS) were used to etch and modify the surface simultaneously. Then, the substrate was polished and cleaned. At a stable temperature of 30 °C, HF solution was present. Then, 0–30 mL of H<sub>2</sub>O<sub>2</sub> was added, followed by the cleaned SLS plate being placed inside the beaker. The reaction lasted for an additional 35–110 minutes after the addition of PFOS. The modified SLS was then cleaned and dried. However, different samples were created, varying the three factors: the molar ratio of H<sub>2</sub>O<sub>2</sub> /HF, reaction time and mass ratio of PFOS to HF. At the optimal sample (molar ratio of H<sub>2</sub>O<sub>2</sub>/HF = 0.2/1, reaction time = 50, mass ratio of PFOS to HF 1/100) maximum WCA of 160.57° ± 0.75° and minimum SA of 1.94° ± 0.25° were obtained [81].

### 2.1.3 Electrochemical Etching and Hydrothermal Synthesis

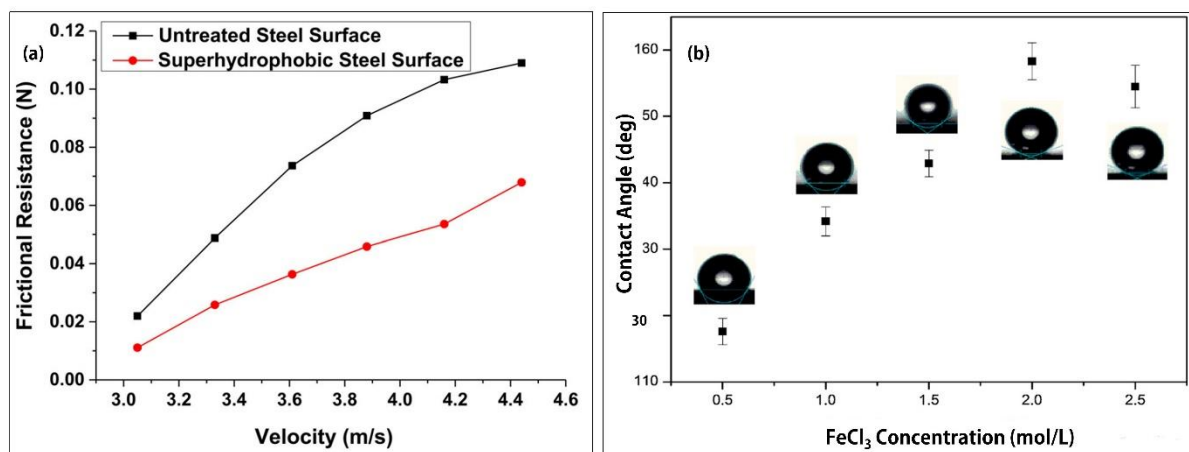
Due to their ability to self-clean and resist corrosion, superhydrophobic surfaces—which exhibit the lotus effect—have a wide range of applications in numerous industries. For a longer shelf life, it is crucial to guarantee the stability of these types of surfaces [82]. Electrochemical etching and hydrothermal synthesis created a stable super-hydrophobic



structure on SS [27]. The author investigated drag reduction for a super-hydrophobic surface in a high-speed fluid and estimated drag reduction at various velocities. Steel foils were polished mechanically and cleaned. Micro/nanoscale hierarchical structures were produced simply through electrochemical and hydrothermal synthesis. The micro-scale structures were fabricated through electrochemical etching in a mixture solution of  $\text{FeCl}_3$  and  $\text{HCl}$ . A two-step process was employed to prepare ZnO nanowires. After that, an ethanol solution containing 0.5 wt.% FAS was used for further modification. However, the concentration of DAP has a significant impact on the water contact angle. **Figure 5** (a) shows that a super-hydrophobic surface reduces drag by about 40–50% at low speeds compared with an untreated steel surface [27].

#### 2.1.4 Chemical Immersion

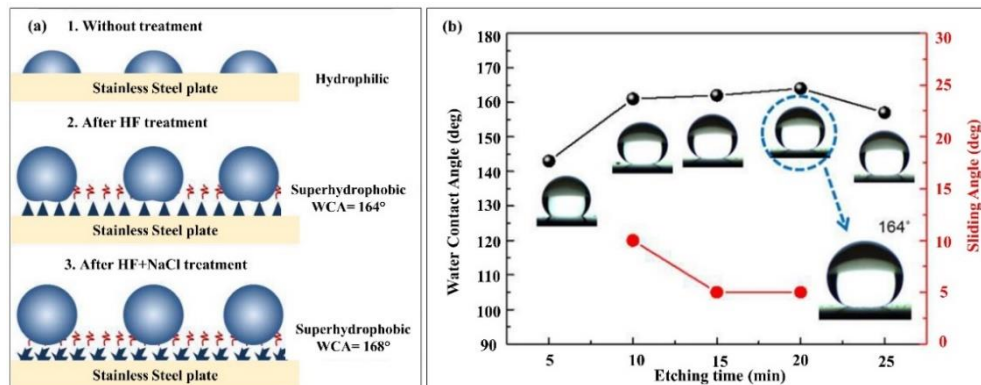
The frosting would occur before icing in colder climates, speeding up the process of icing formation and development. As a result, the anti-icing application of superhydrophobic surfaces relied on the anti-frosting feature [83]. Achieving the anti-frosting property of the superhydrophobic surface is the main target of this research [42] and so a highly effective and low-cost biomimetic superhydrophobic surface on 304 SS was developed through a chemical immersion process. Firstly, the substrate was polished with sandpaper and then cleaned. After that, micro/nanoscale roughness was created on the SS surface by chemically etching in FHH solution ( $\text{FHH FeCl}_3 + \text{HCl} + \text{H}_2\text{O}_2$ ), then the surface was modified with DTS. It has been found that the concentration of  $\text{FeCl}_3$  in the FHH solution impacted superhydrophobicity. With the increased concentration of  $\text{FeCl}_3$  in the FHH solution, the surface microstructure density changed gradually, enhancing the super-hydrophobic property [42]. Moreover, besides  $\text{FeCl}_3$  concentration, several other factors determine the SS morphology, such as etching time, etchant composition, the characteristics of the metal being etched, and so forth. 20 min etching time and FHH solution with 2mol/L  $\text{FeCl}_3$  are the optimal conditions for achieving the greatest WCA of  $158.3^\circ \pm 2.8^\circ$  after DTS modification, as shown in **Figure 5** (b) [42].



**Figure 5:** (a) Friction drag vs. velocity of water flowing over surfaces [27], (b) Contact angles at different  $\text{FeCl}_3$  concentration [42].

#### 2.1.5 Two-step Etching

The self-cleaning property is an essential feature of super-hydrophobic surfaces, and this property can be achieved through several processes. The author of [51] used a simple two-step chemical etching technique to produce a super-hydrophobic surface with good durability and self-cleaning capability. Firstly, the stainless-steel substrates were cleaned, and a micro-nano structure was created after etching. HF was used as etching solution. This modified surface was dipped into a 0.1 wt.% NaCl solution to generate superhydrophobicity. This dipping into NaCl enabled nano-scale roughness to be induced and formed micro-nano hierarchical structures. For fluorination, hexane containing PFOS was used. **Figure 6** (a) shows the schematic of two-step chemical etching for fabricating SHS. It is evident from **Figure 6** (b) that 20 minutes of HF etching followed by a 3-hour NaCl dip (0.1 wt.%) was most effective in achieving superior hydrophobic performance [51].

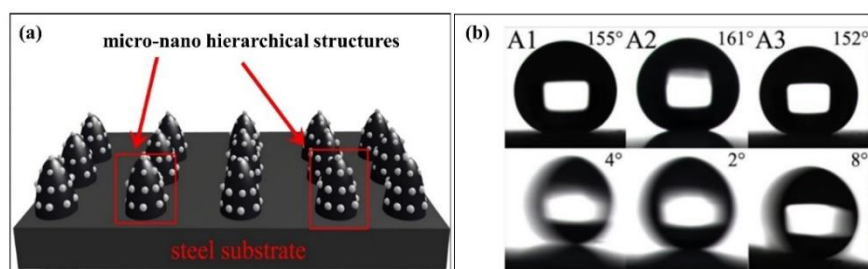


**Figure 6:** (a) Schematic diagram of the hydrophobicity state of the stainless steel sample [51], (b) Effect of HF etching time variation on the surface wettability and sliding behaviour of stainless steel [51].

This article [54] suggested a two-step chemical etching process for creating super-hydrophobic surfaces on stainless steel substrates. The samples were first polished and successively submerged in HCl solution and  $\text{FeCl}_3$  solution to obtain microstructure. In the first two chemical etching stages, the samples were submerged in an HCl solution for varying etching periods (10 to 55 min) and concentrations (1 to 8 mol/L). In the second phase, they were submerged in a ferric chloride solution for etching periods ranging from 1 to 8 hours, concentrations ranging from 0.5 to 25 weight percent, and temperatures ranging from 25 °C to 112 °C. For 30 minutes, the etched samples were submerged in a 0.1 wt.% fluoroalkyl silane solution. However, etching in a solution of 5 mol/L HCl for 25 min, immersion in a solution of 1 wt.%  $\text{FeCl}_3$  at 100 °C for four hours, and then fluoroalkyl silane modification led to a maximum WCA of 159° and a minimum SA of 2°. In another study [84], the SS plates were immersed in a 38% ferric chloride solution for microstructure formation and in a 34.5% hydrogen peroxide solution for surface oxidation. Etching and oxidation of STS316L achieved a superhydrophilic state, which was reversed to superhydrophobicity with an Heptadecafluoro-1,1,2,2-tetrahydrodecyl trichlorosilane (HDFS) coating, resulting in a contact angle of 168° and superior performance in self-cleaning tests.

### 2.1.6 Etching for Anti-icing

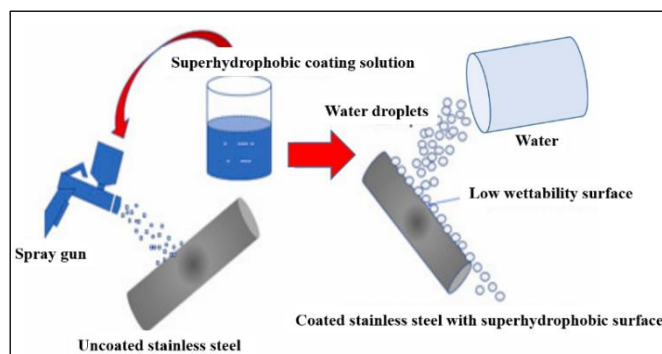
Anti-icing characteristics of super-hydrophobic surfaces have been discovered in recent years by researchers. These surfaces can significantly lessen the icing adhesion force and prolong the icing process [85], [86]. The super-hydrophobic surface was made using a simple approach that involved mixing  $\text{H}_2\text{O}_2$  and  $\text{H}_2\text{SO}_4$  to create flower-like hierarchical structures and then treating them with silanes. The primary goal of this research [87] was to get the prepared surface to have anti-icing properties. Firstly, the pretreated substrates were etched by  $\text{H}_2\text{SO}_4$  and  $\text{H}_2\text{O}_2$  mixed solution to get microstructure. The samples were then immersed into 5wt. % HDTMS (sample A1), 1H, 1H, 2H, 2H-perfluorodecyltriisopropoxysilane (FAS-17) (sample A2), and MTMS (sample A3) in hexane to modify the surface with low-energy components. The synthesized SHS contains micro-nano hierarchical structures (Figure 7 (a)), and all the prepared samples had very low adhesion ( $\text{SA} < 10^\circ$ ) and high CA values ( $> 150^\circ$ ), as shown in Figure 7 (b) [87]. So, FAS has the lowest surface free energies, then hexadecyltrimethoxysilane (HDTMS), and finally methyltrimethoxysilane (MTMS). As a result, the FAS-modified surface had greater CA and lower SA values.



**Figure 7:** (a) An illustration of the hierarchical structures, (b) The prepared surface wetting characteristics for different reagents [87].

### 2.2 Coating

A coating is a protective layer applied to an object's surface [88]. Several surface characteristics, including wettability and adhesion, can be improved by functional coatings. Furthermore, coatings can increase wear and corrosion resistance [89], [90]. However, the coating can also provide super hydrophobicity on substrates, as shown in Figure 8 [91]. Various coating methods, such as sol gel/ dip coating, spin coating, spray coating can make stainless steel substrates superhydrophobic.

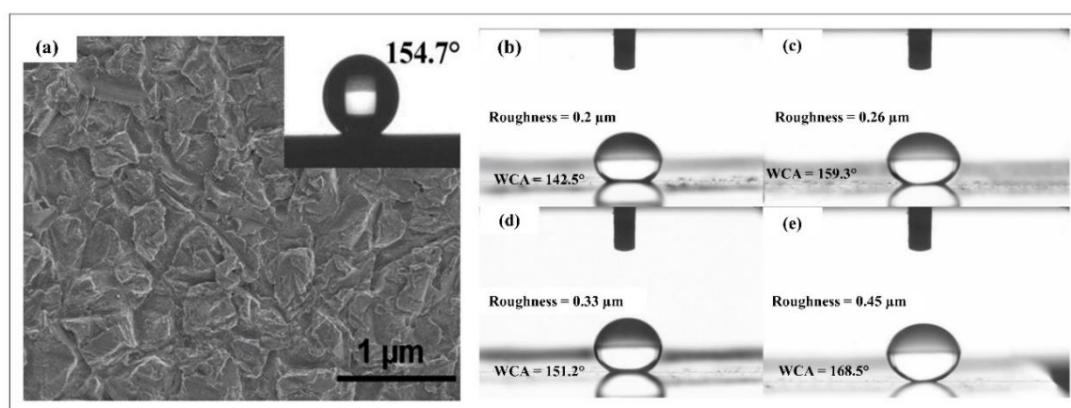


**Figure 8:** Schematic representation of coating on stainless steel for super hydrophobicity. (Regenerated from [91])

### 2.2.1 Sol Gel and Dip Coating

One of the essential properties of super-hydrophobicity is its capacity to resist corrosion in corrosive settings while preserving its chemical stability and super-hydrophobic properties. Using the sol-gel process and the dip-coating technique, the author [43] fabricated a nano-structured  $\text{SiO}_2$  coating on stainless steel to achieve super-hydrophobicity with excellent corrosion resistance. The stainless-steel sheet was mechanically polished and cleaned. Tetraethyl orthosilicate (TEOS) and ethanol were used for  $\text{SiO}_2$  sol preparation. The sample that had been pre-treated was dipped in  $\text{SiO}_2$  sol, dried, and then annealed. The annealed specimen was placed into a 1.0 wt.% ethanol solution of FAS and heated later. Thus, a rough surface was created by the  $\text{SiO}_2$  coatings, which comprises “island” structures. The  $\text{SiO}_2$  coating exhibits good super-hydrophobicity with a water contact angle of  $154.7^\circ$  following FAS modification, as shown in **Figure 9** (a) [43].

A critical factor in achieving super-hydrophobicity is surface roughness. It significantly impacts the contact angle. Hydrophobicity, as measured by CA level, improved with surface roughness. Investigations were conducted into the effects of surface roughness and super-hydrophobicity of  $\text{TiO}_2$  thin films on the surface of 316L stainless steel substrates produced using the sol-gel/dip-coating process [92]. As a titanium source, titanium (IV) isopropoxide (TTIP) was chosen to synthesize  $\text{TiO}_2$  sol. By dipping-withdrawing, thin coatings were applied to the produced sol solutions on the stainless-steel substrates. The surface had a homogeneous, very dense nanocrystalline  $\text{TiO}_2$  covering as the surface roughness increased. Since all  $\text{TiO}_2$  thin films have the same chemical characteristics, the difference in wettability across the samples was often determined by how rough the surface was, and rougher surfaces resulted in more hydrophobic behaviour and less wettability. The impact of surface roughness on the wettability characteristics of the surfaces is shown in **Figure 9** (b) [92]. It was revealed that although there was a tiny change in the roughness ( $0.25 \mu\text{m}$ ), the water contact angle changed dramatically, rising to  $26^\circ$ .

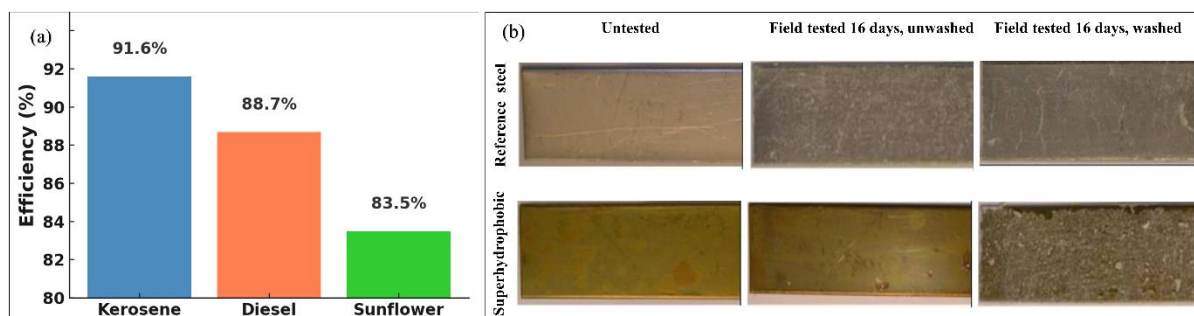


**Figure 9:** (a) SEM view of  $\text{SiO}_2$  coating and water contact angle after modified with FAS [43], (b-e) The impact of surface roughness on the wettability characteristics of the surfaces. (Regenerated from [92])

The health of people and the sustainability of the environment are at risk worldwide due to oil-contaminated water resulting from industrial waste or oil spill disasters. With high separation efficiencies for kerosene and diesel, a low-cost and effective  $\text{TiO}_2$ /PDMS-coated mesh with superhydrophobic and superoleophilic qualities presents a viable option for tackling the global problems caused by oil-contaminated water. The process of dip coating was used to fabricate the superhydrophobic  $\text{TiO}_2$ /PDMS [93]. The coated mesh exhibited a water contact angle (WCA) of  $155^\circ$  and an oil contact angle (OCA) of  $0^\circ$ , indicating its unique superhydrophobicity and superoleophilicity. As illustrated in **Figure 10** (a), the separation efficiencies for diesel and kerosene were determined to be 88.7% and 91.6%, respectively [93].

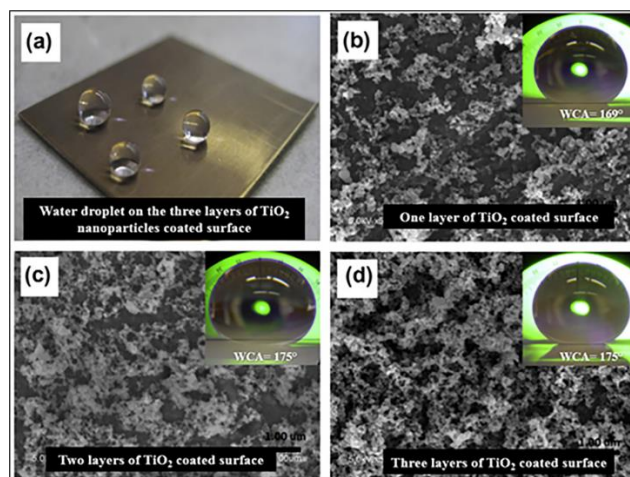
### 2.2.2 Spin Coating

Surfaces are given the appropriate self-cleaning qualities by coating. However, in some cases, coated finishes may be needed for stainless steel structures or components. The main objective of this research [94] was to fabricate a Flaky  $\gamma$ -alumina coating on SS substrate that would show easy-to-clean properties with excellent durability. Al and isopropyl alcohol were combined to create a flaky  $\gamma$ -alumina coating. However, the cleaned substrate was spin-coated for 20 seconds at 1500 rpm. The coated sample was heated after being submerged in the FAS solution for one hour. **Figure 10** (b) shows the easy self-cleaning property of the as-prepared SH sample. The maximum WCA of untested superhydrophobic SS, field-tested superhydrophobic SS, and uncoated reference SS after a 16-day run was  $150^\circ$ ,  $124^\circ$ , and  $74^\circ$ , respectively [94]. The minimum and maximum WCA values after washing the under-tested coated sample later in the six-week run were  $79^\circ$  and  $122^\circ$ , respectively.



**Figure 10:** (a) Separation efficiency of different oil (regenerated from [93]), (b) The photographic views of untested and field tested samples [94].

Superhydrophobic surfaces can resist corrosion in corrosive environments while maintaining chemical stability and UV resistance properties. A simple and inexpensive layer-by-layer deposition process was utilized to induce superhydrophobicity on stainless steel substrate using  $\text{TiO}_2$  nanoparticles [44]. A precursor three layer of Poly(diallyldimethylammonium) (PDDA) and poly (sodium 4-styrenesulfonate) PSS was initially applied to the cleaned substrate. After that, the substrates were alternately submerged in  $\text{TiO}_2$  P25 aqueous solution and PSS aqueous suspension for creating multilayer films of  $\text{TiO}_2$ /PSS. A 1H,1H,2H,2H-perfluorodecyltriethoxysilane (PFES) was then used to treat the samples. The UV protection layers were applied by alternately dipping the as-prepared coatings in PDDA aqueous solution and  $\text{SiO}_2$  aqueous solution. The wetting behaviour of the prepared different layer-coated surfaces is shown in **Figure 11** [44].



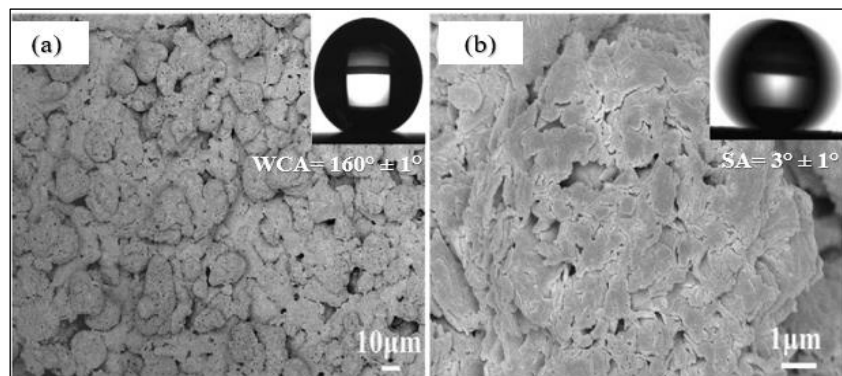
**Figure 11:** (a) Water droplets on the treated steel surface, SEM images and wetting behaviour of  $\text{TiO}_2$  nanoparticles coated SS surface of (b) Single-layer  $\text{TiO}_2$  coating, (c) Double-layer  $\text{TiO}_2$  coating and (d) Triple-layer  $\text{TiO}_2$  coating (Regenerated from [44])

### 2.2.3 Spray Coating

Damage or oil fouling can be minimized by including easy reparability into the superhydrophobic surface, which is assumed to meet future demands in practical applications. A facile and effective spray-coating method created superhydrophobic surfaces on almost any substrate. The primary goal of this research [95] was to create superhydrophobic surfaces on various substrates using a one-step spray-coating process, which eliminated the complexity of two different phases in traditional methods while allowing for easy reparability. This process used a traditional

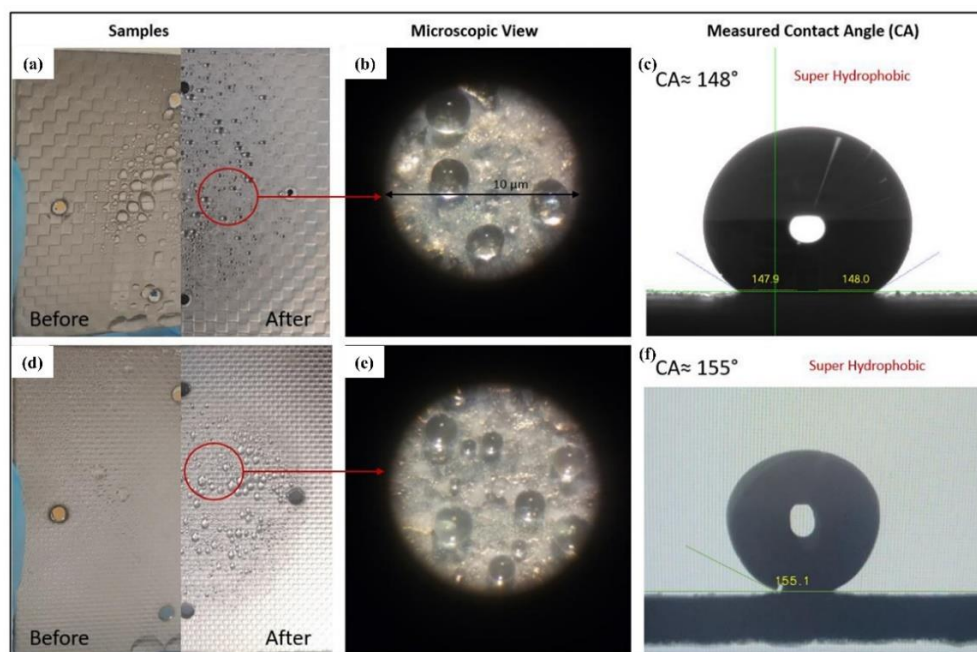


precipitation approach to create copper stearate. After dispersing the produced copper stearate in ethanol, a spray gun was used to apply the suspension to the samples. The coating was dried at room temperature. The water contact angle and sliding angle on the surface were  $160^\circ \pm 1^\circ$  and  $3^\circ \pm 1^\circ$ , respectively, as shown in **Figure 12**, meaning water droplets had little adhesion to it [95].



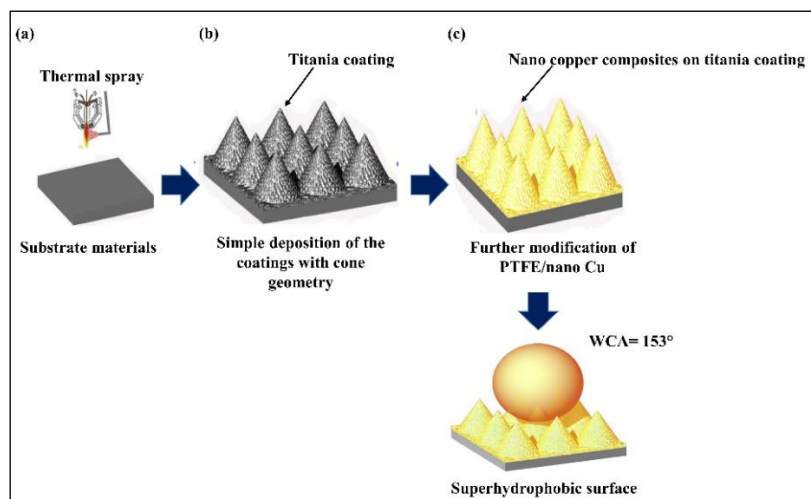
**Figure 12:** FE-SEM images of the as-prepared super hydrophobic surface at (a) 10  $\mu\text{m}$ , (b) 1  $\mu\text{m}$  [95].

Atmospheric water generation (AWG) produces drinkable water by using the surrounding air. As a result, it can address the issues with fresh drinking water [96]. Ice build-up on the condensation surface and the device's generally low efficiency are challenges in this research [97]. hydrophobic coating on stainless steel formed a superhydrophobic surface to minimize the issue, improving dropwise condensation and condensation droplets from the surface. Isopropanol was used to wash the sample surfaces, which were thoroughly dried, to remove contamination. After applying three coats, the samples were allowed to dry for 30 minutes. A commercially available super-hydrophobic was used to coat the commercial grade SS and produced super-hydrophobicity on SS, depicted in **Figure 13** [97]. A superhydrophobic surface has been found to promote dropwise condensation, and condensate droplets exit from that surface. The surface itself is exposed to promote the development of new droplets since the drops in this condensation process are discrete, continuously created, and released from the surface.



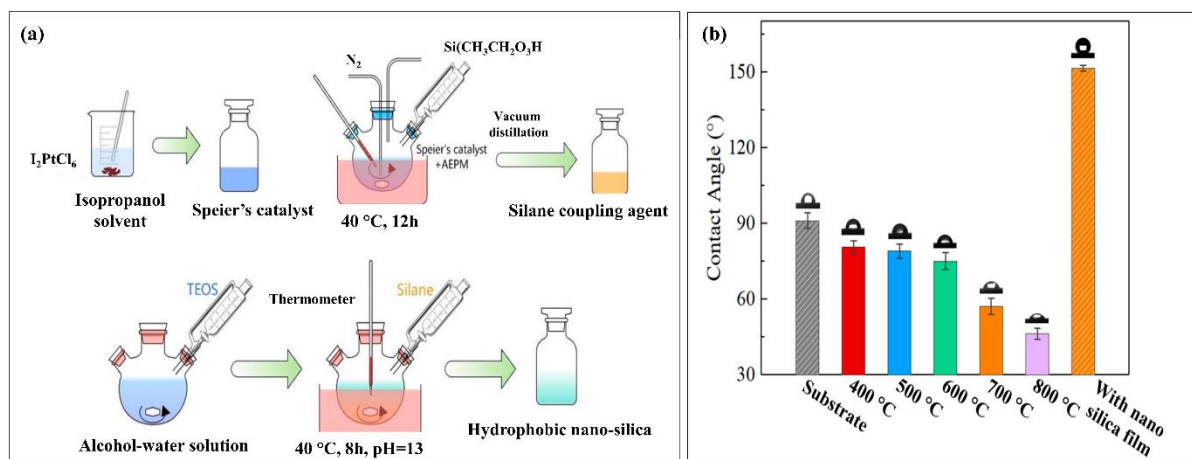
**Figure 13:** (a-f) Samples showing photographs of wettability behaviours before/after applying the hydrophobic spray [97].

The author of [98] showed how to make super-hydrophobic surfaces that are physically strong and repairable using a thermal spray method. Plasma spray was used to create patterned titania coatings with cone-like geometry. Further modification was done with PTFE/nano-Cu as a top layer on the substrates. The coatings were deposited by atmospheric plasma spray on stainless steel plates (316L) and increased the hydrophobicity (**Figure 14**) [98]. Micro-patterned topographical features of the coatings were achieved.



**Figure 14:** (a-c) The steps involved in creating a superhydrophobic surface using the thermal spray technique. (Regenerated from [98])

High-temperature oxidation in conjunction with a nano-silica coating was found to be a sustainable way to create coloured superhydrophobic stainless steel surfaces with improved corrosion resistance and self-cleaning capabilities [99]. The coloured stainless-steel surface was sprayed with the silica suspension. The preparation of hydrophobic nano-silica is shown in **Figure 15** (a). Following that, heat treatment was applied to the sprayed surface to produce a superhydrophobic stainless steel coating. The coloured surface was more corrosion-resistant and had superhydrophobic qualities compared to the coloured stainless-steel surface with the oxide coating and substrate. The contact angles of oxide films created at various oxidation temperatures and the oxide film formed at 800 °C after being treated with the superhydrophobic nano-silica film are shown in **Figure 15** (b) [99]. The surface contact angle significantly decreased as the oxidation temperature rose. A significant increase in surface wettability was demonstrated by the contact angle, which reached  $46.2^\circ \pm 2.2^\circ$  at 800 °C. Nevertheless, the contact angle of the treated sample was  $151.5^\circ \pm 1.2^\circ$  after the oxide layer that had developed at 800 °C was treated with the superhydrophobic nano-silica film.



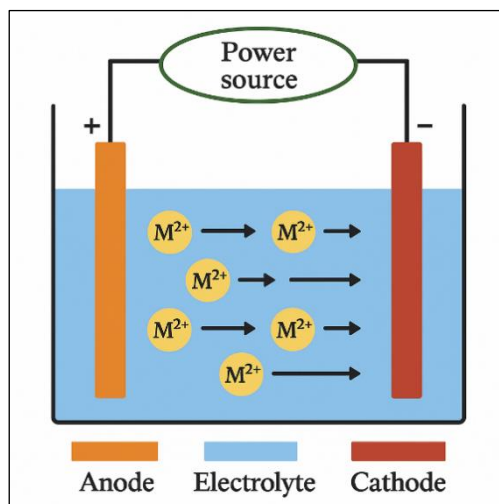
**Figure 15:** (a) Hydrophobic nano-silica preparation, and (b) the relation between the contact angle at various oxidation temperature and oxide film with superhydrophobic nano silica film [99].

The long-standing problem of inadequate durability in industrial applications is addressed by this study [100], which offers an economical and ecologically responsible approach to creating mechanically strong superhydrophobic surfaces with remarkable water repellence and abrasion resistance. The hydrophobic suspension of  $SiO_2$  nanoparticles was sprayed onto substrates that had been treated with adhesive. The coated substrates exhibit extremely low water adhesion (contact angle  $\approx 160^\circ$  and slide angle  $< 2^\circ$ ) and outstanding superhydrophobic qualities. Furthermore, even after 325 sandpaper abrasion cycles, the coated surface retained its superhydrophobicity, demonstrating exceptional mechanical robustness. Moreover, a 3D-printed micro-structured surface, modified with a low-surface energy substance, demonstrates exceptional superhydrophobic properties and advanced performance in droplet freezing and impact tests, highlighting its potential for applications requiring enhanced water repellence and durability. To

create a cross-floral structure model, this study used Bessel curves and circular arc curves. Using a low-surface-energy substance called Ultra-Ever Dry to alter the wettability of the micro structured surface, the superhydrophobic surface was created by spraying [101]. After application, the wettability of the surface increased dramatically, achieving a contact angle of  $153.7^\circ$ . The cross-shaped biomimetic structure designed by the Bessel curve revealed a maximum droplet freezing time of 4193 s and a minimum droplet impact time of 9.81 ms.

### 2.3 Electrochemical Deposition

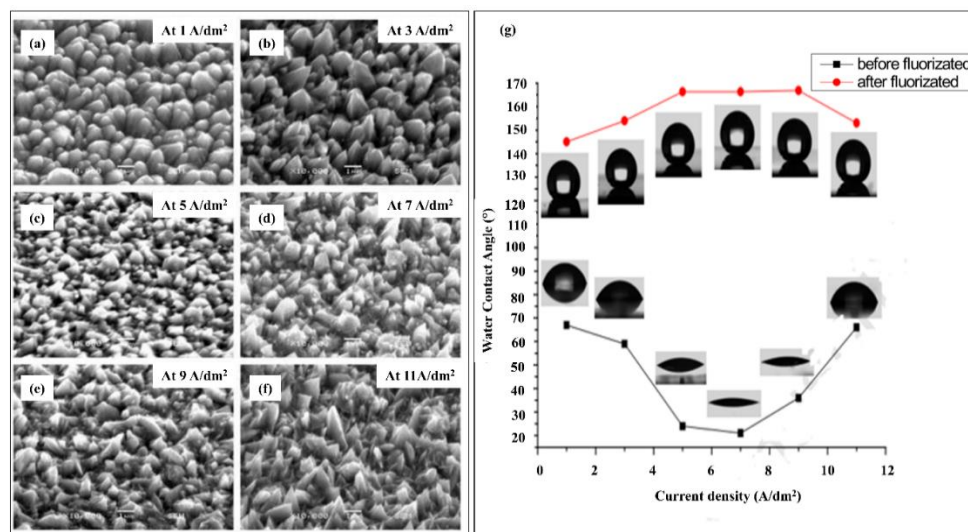
Electrochemical deposition is the process of depositing one material onto the surface of another through oxidation and reduction. It has the potential to form thin layer deposits that, with some modification, make the surface superhydrophobic. It is a cost-effective method and can alter the surface property of metal [102], [103]. A schematic of electrodeposition process is illustrated **Figure 16** [104].



**Figure 16:** Schematic of an electrodeposition process for metals. (Regenerated from [104])

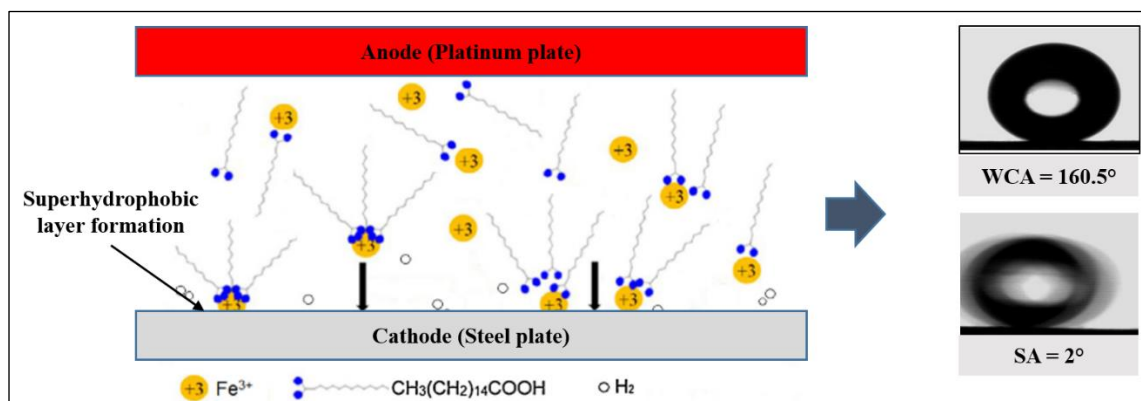
#### 2.3.1 Electrodeposition

The key properties of super-hydrophobic surfaces are stability and corrosion resistance. This research [45] used a combination of electrodeposition and fluorinated modification techniques to obtain these key features on the SS 316L substrate. The SS 316L sheets were initially cleaned, and the oxidation layer was removed. The cathode and anode plates were submerged in electrolytic solutions. A nickel film was electro-deposited on SS 316L substrates by a DC power supply. The SS 316L sheets were electroplated and then fluorinated by dipping them into a 2-weight percent FAS-13 solution. The surface of the electrodeposited nickel film has various micro/nanostructures at different current densities due to the cathodic polarization, as shown in **Figure 17** (a-f). Before fluorinating the nickel sheets, the contact angle was highest ( $65^\circ$ ) at low ( $1\text{--}3\text{ A/dm}^2$ ) or high ( $11\text{ A/dm}^2$ ) current densities. At a current density of  $5\text{ to }9\text{ A/dm}^2$ , FAS-13 modification may cause the deposited surface to change into a superhydrophobic surface (CA of  $165^\circ$ ) as shown in **Figure 17** (g) [45].



**Figure 17:** (a-f) The surfaces images of the electrodeposited nickel film at various current densities, (g) The relation between the water contact angle and electrodeposition current density. (Regenerated from [45])

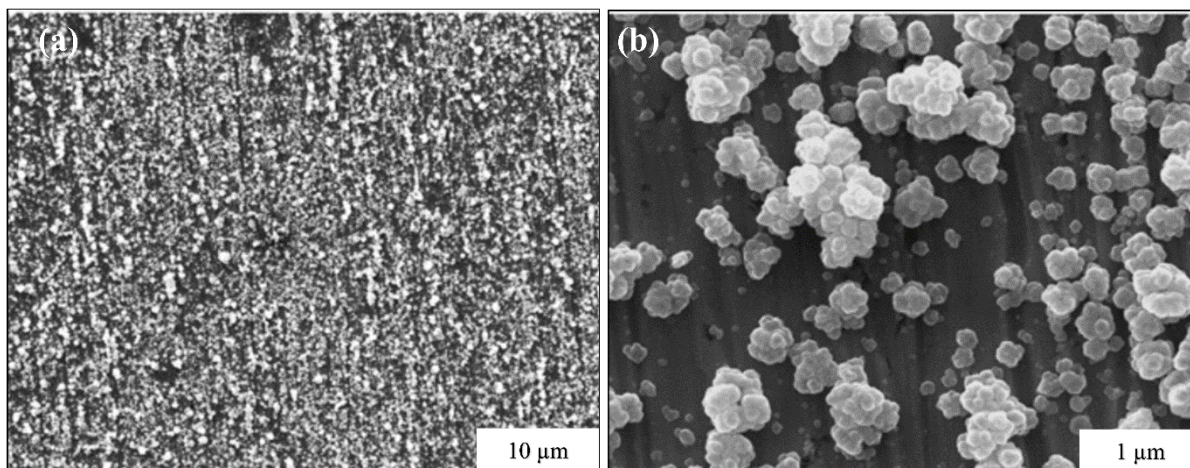
Being an active metal, carbon steel has an innate difficulty with corrosion. Surface coating technology is an excellent approach for protecting steel from corrosion. The author [105] described a simple and one-step electrochemical deposition procedure for creating a super-hydrophobic coating on steel surface with robust anti corrosive property. A platinum wire and steel sheet functioned as anode and cathode in a two-electrode cell. The film was deposited in ferric chloride/palmitic acid/ethanol solution. In this technique, a WCA of  $160.5^\circ \pm 0.5^\circ$  and a sliding angle of  $2^\circ \pm 0.5^\circ$  were achieved as shown in **Figure 18** [105]. After immersing the prepared surface in water for seven days, it was found that CA had decreased from  $161^\circ$  to  $156^\circ$  and SA had grown from  $2^\circ$  to  $6^\circ$ .



**Figure 18:** Wettability behaviour of the as prepared superhydrophobic surface. (Regenerated from [105])

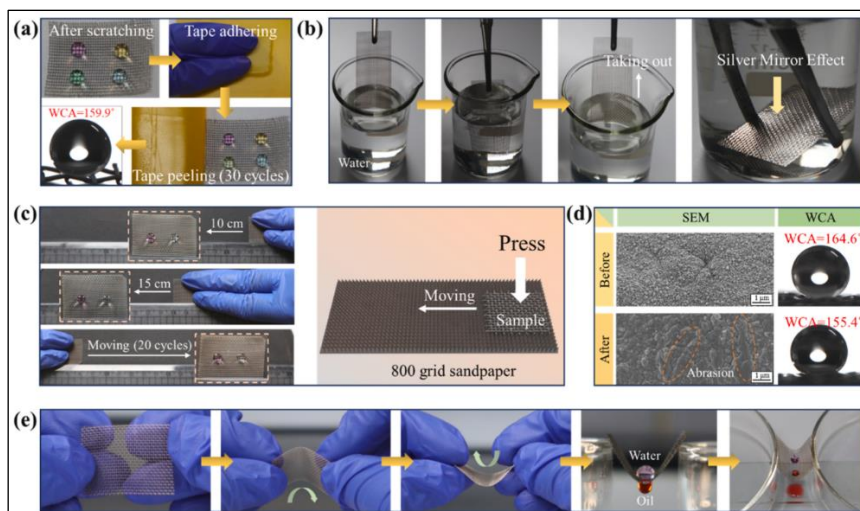
Superhydrophobic surfaces on 316L stainless steel were created using a quick process that involved electrolyzing the metal [106]. For this purpose, lauric/nickel chloride/ethanol solution was utilized. The sample experienced etching for 900 s. After the sample had been cleaned, it was submerged in a uniform ethanol-based nickel chloride and lauric acid electrolyte solution. The samples served as the cathode and anode, and a DC voltage was applied between them. Then the working electrodes were cleaned after the chosen electrolysis duration and dried in the air to provide the cathodic surface as superhydrophobic. It was revealed that 30 s of reaction was enough to obtain a superhydrophobic surface with a maximum WCA of  $175^\circ$ . **Figure 19** shows the SEM images of the prepared superhydrophobic coating after 30 s [106].





**Figure 19:** SEM images of the superhydrophobic surface coatings for 30s reaction time; (a) 10  $\mu\text{m}$  and (b) 1  $\mu\text{m}$  [106].

Oil pollution in aquatic systems is an environmental problem that can be solved by creating long-lasting, superhydrophobic-superoleophilic materials such as nickel palmitate stainless steel meshes (SNP-SSM). Thus, it is very desirable to produce a high-flux, long-lasting material for separating oil-water mixtures. This study proposed a novel one-step electrodeposition process for creating superhydrophobic-superoleophilic nickel palmitate stainless steel meshes (SNP-SSM). A superhydrophobic micro/nanostructure was electrodeposited in the electrodeposition precursor solution at 60 °C using the pre-cleaned stainless-steel mesh and Ti-IrO<sub>2</sub> sheet as cathode and anode right away. This resulted a superhydrophobic stainless steel mesh after a 14-minute reaction. A water contact angle (CA) of  $164.98^\circ \pm 2.3^\circ$  and a roll-off angle (ROA) of  $4.78^\circ \pm 1.3^\circ$  are displayed by the SNP-SSM. Additionally, the SNP-SSM demonstrates adequate mechanical, chemical, and thermodynamic resistance in a variety of tests, as illustrated in **Figure 20** [107].



**Figure 20:** Investigations of mechanical robustness of eSNP<sub>CIT</sub>. (a) Optical images of eSNP<sub>CIT</sub> following knife scratch and adhesive tape cyclic peeling tests, (b) Repeated immersion experiment and silver mirror effect, (c) cyclic sandpaper abrasion test, (d) SEM images and contact angle before and after sandpaper abrasion, (e) Bending durability test under cyclic loading conditions [107].

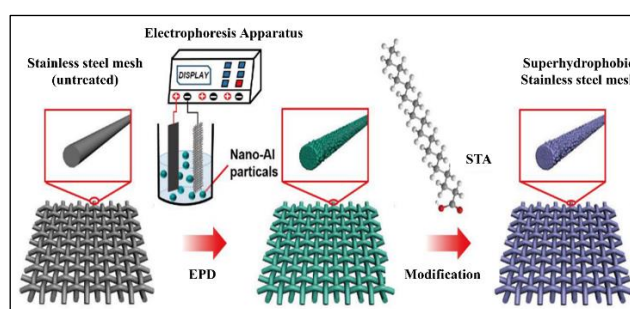
Inspired by natural antifouling surfaces, superhydrophobic stainless-steel meshes containing antibacterial silver nanoparticles, created via electrodeposition and surface modification, successfully inhibit *S. aureus* adherence, especially in static environments. The stainless-steel mesh was utilized as the working electrode in a three-electrode deposition system, which was employed to electrodeposit Ag nanoparticles onto the SS mesh at room temperature in an aqueous electrolyte containing AgNO<sub>3</sub>, sodium citrate, and KNO<sub>3</sub>. Stainless-steel meshes modified by PDA@ODA compounds exhibited a superhydrophobic condition with a SA of 3° and a CA of 160.6°. In static culture, the superhydrophobic specimens were able to efficiently reject *S. aureus* adhesion, showing a more noticeable effect than in dynamic conditions [66].

Examining the effects of scan rate and limitations on improved protection in acidic conditions, the study investigates the electrochemical deposition, thermal stability, and corrosion resistance of polyaniline coatings on 316L

stainless steel. Using thermogravimetric analysis, the thermal stability of the PANI coating was assessed, and electrochemical impedance spectroscopy (EIS) was used to examine the corrosion behaviour of coated and bare steel in 1M  $\text{H}_2\text{SO}_4$ . 316L stainless steel served as the working electrode, Pt served as the counter electrode, and Ag/AgCl served as the reference electrode. EIS Nyquist plots demonstrated that the PANI coating's corrosion resistance increased considerably with lower scan rates and a smaller upper potential, particularly after up to 72 hours of exposure [108].

### 2.3.2 Electrophoretic Deposition

Employing superhydrophobic meshes as an oil and water separator in the petroleum industry and other associated sectors is quite feasible. The author [47] demonstrated super-hydrophobic nano Al films on stainless steel meshes fabricated via the electrophoretic deposition (EPD) process, expecting to provide a cost-effective method for promising practical applications in oil-water separation. A stable suspension was created by using Al particles. The EPD procedure was conducted at room temperature with an operating voltage of 10  $\text{V}\cdot\text{mm}^{-1}$ . Subsequently, the cathode samples were meticulously cleaned. At last, they were dipped into a 5% ethanol solution and allowed to dry. This approach yielded a WCA of  $160^\circ \pm 1.2^\circ$  and a WSA of less than  $5^\circ$ . **Figure 21** shows the schematic illustration of EPD fabrication process [47].



**Figure 21:** Schematic illustration of EPD fabrication [47].

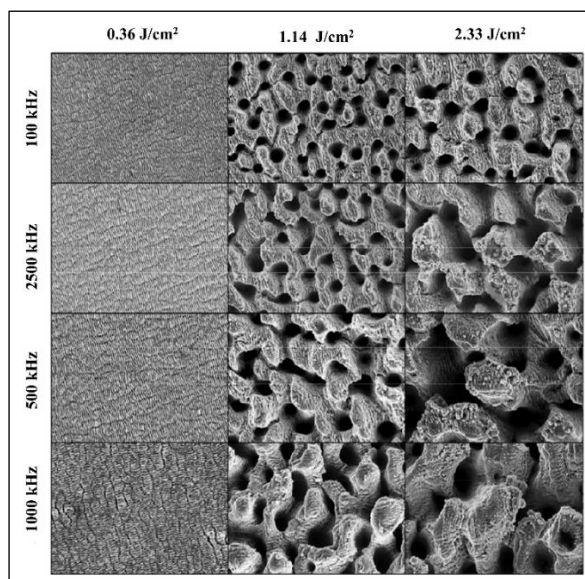
## 3. Mechanical Process

Any action or procedure conducted by a machine is referred to as a mechanical process. A mechanical process may also be described as a process that is made, carried out, operated by, or connected with machinery, related to, controlled by, or operated by physical forces [109]. Superhydrophobic surfaces have recently gained increased attention due to their potential utility in self-cleaning, anti-icing, reducing drag, and resisting corrosion. The primary method for creating superhydrophobic surfaces involves creating microstructures and then applying a coating material to reduce the surface energy. However, mechanical techniques like heating, thermal spraying, and laser texturing can also create super-hydrophobic surfaces.

### 3.1 Laser Texturing

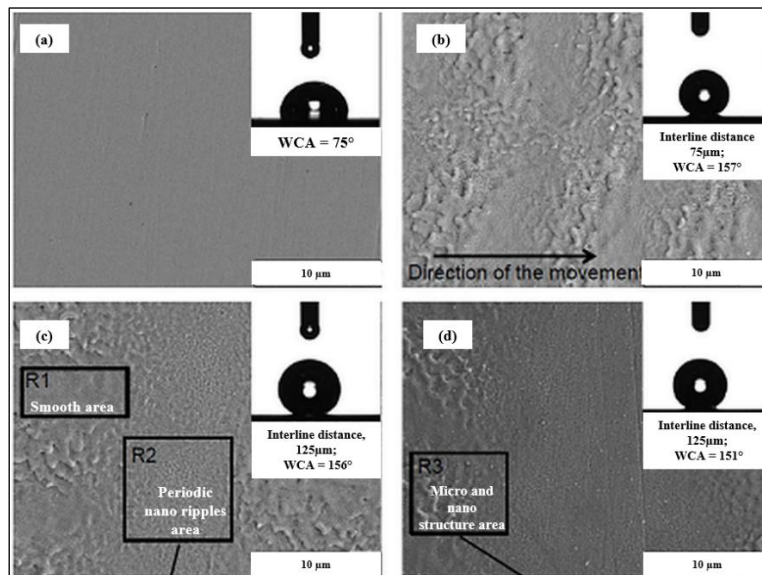
One amazing method for altering a material's surface quality is laser texturing. Furthermore, it can significantly alter the roughness and texture of the material. The laser beam forms micro-patterns on the surface. Moreover, it has excellent repeatability and micrometer accuracy when eliminating layers. Laser surface texturing can enhance several essential characteristics, including adhesion, wettability, and friction. In addition to enhancing mechanical seal performance, laser texturing can prepare surfaces for laser cladding and thermal spraying [110].

This study [49] used a high average-power and high repetition-rate femtosecond laser to create superhydrophobic surfaces on AISI 316L steel to fully utilize the laser system's capabilities while reducing the overall process takt-time. The optimum superhydrophobic characteristics were attained by varying the laser's energy and repetition rate. A 316L steel sample was mirror-polished, and a femtosecond laser was employed to obtain a superhydrophobic surface. Four different repetition rates were investigated, namely 100 kHz, 250 kHz, 500 kHz, and 1000 kHz. For each repetition rate, the energy per pulse was varied accordingly to reach fluence per pulse, ranging from  $0.36\text{J}/\text{cm}^2$  to  $2.33\text{J}/\text{cm}^2$ . Laser-induced periodic surface structures (LIPSS) were observed at low fluence per pulse, and with increasing repetition rate, micro-grooves structure of spatial periodicity was observed. As the fluence per pulse and repetition rate increases, the structure changes from a highly homogeneous net of circular holes to columnar structures, removing nano features later. **Figure 22** shows the SEM views of steel surfaces after laser texturing with different fluence per pulse and repetition rate [49]. The hydrophobic behaviour is seen in the low fluence domain after several days at a low repetition rate (100kHz - 250kHz). The highest CA values are obtained at low fluence per pulse in the high repetition rate (500kHz–1000kHz) just a few days after the laser processing. This is due to the nano-features (LIPSS) and micro-groove structure. The increase of the CA values in time is faster at higher repetition rates superhydrophobic surfaces ( $\text{CA} > 150^\circ$ ) are obtained already after ten days from the day of the laser processing for several values of fluence per pulse [49].



**Figure 22:** SEM images of 316L steel surfaces after laser texturing with different at fluence per pulse and repetition rate [49].

Femtosecond laser treatment was used [111] to modify the surface chemistry and topography of stainless steel plates with the aim of improving osseointegration. Micro-spotted lines separated by different nanostructured interline (75, 125 and 175  $\mu\text{m}$ ) on stainless steel were created using a femtosecond laser treatment. This work sheds light on the potential applications of femtosecond laser-treated surfaces in preventing or reducing aseptic loosening and osteolysis. An ultrashort laser was used to treat the sample's surfaces. Maximum CA ( $157^\circ$ ) was obtained for an interline distance of 75  $\mu\text{m}$  as shown in **Figure 23** [111]. At a spacing of 125  $\mu\text{m}$  between lines, the maximum bone mineral accumulation was observed on the surface.

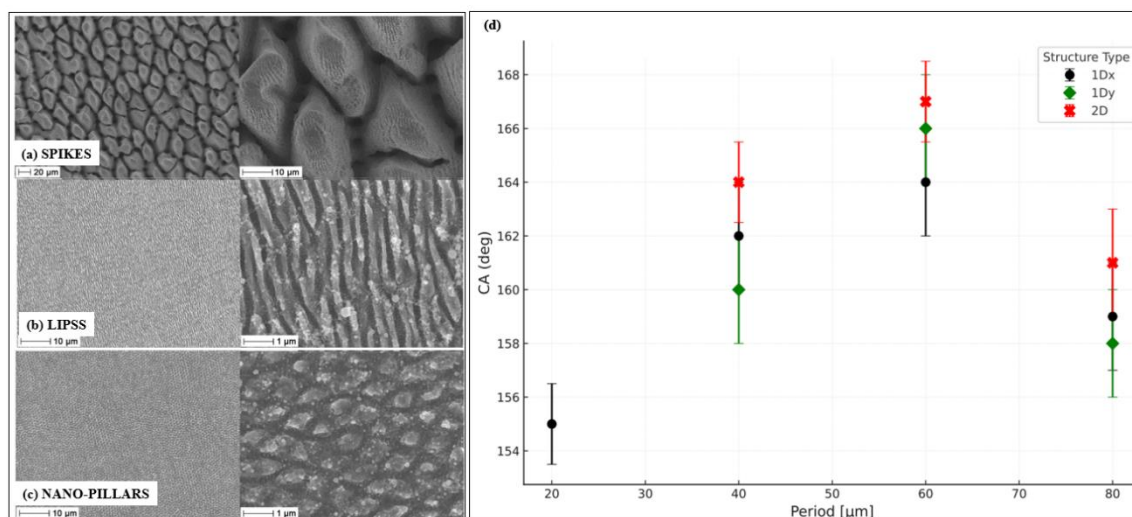


**Figure 23:** SEM images and water contact angles of the (a) untreated and (b-d) laser treated samples. (Regenerated from [112])

The laser-textured antibacterial surface on stainless steel was fabricated using a femtosecond laser [113]. Antibacterial performance was measured by quantifying the retention of *Escherichia coli* and *Staphylococcus aureus* germs on surfaces textured by ultrashort pulse laser and mirror polishing. After polishing the sample, laser irradiation was conducted. As illustrated in **Figure 24** (a), LIPSS, spikes, and nano-pillars were created for every specimen [113]. After being exposed to the atmosphere for 30 days, the hydrophilic spike structures that were created turned superhydrophobic ( $\text{CA}=160^\circ$ ). The study found that implementing LIPSS and nano-pillar structures can significantly lower the retention of *E. coli* by 99.8% and 99.2%, respectively, and *S. aureus* by 84.7% and 79.9%.



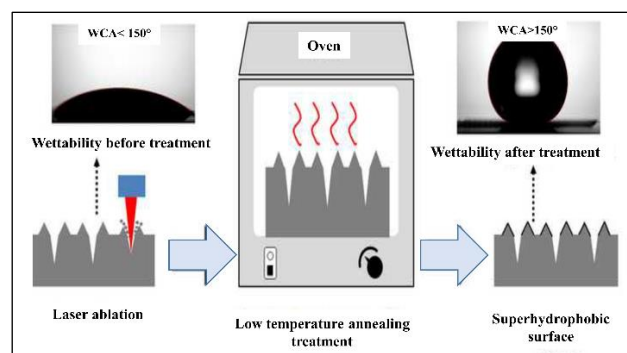
Superhydrophobic surfaces were synthesized by laser ablation with the addition of silanization in many studies. However, the primary purpose of this study [114] was to use femtosecond laser machining in the open air to generate micro and nano-scale patterns with hydrophobic qualities without any extra post-treatment. For specific samples, laser texturing was conducted along a single axis with periods varying from 20 to 80  $\mu\text{m}$ . In contrast, the laser was used for other samples to manufacture a grid pattern with 40, 60, and 80  $\mu\text{m}$  periods. It was observed that the surfaces with sixty  $\mu\text{m}$  spacing produce a clear valley-ridge pattern in the case of the one-dimensional scan. Increased spacing further than sixty  $\mu\text{m}$  intuitively leads to less hydrophobicity. The grid pattern performed better than a 1D line pattern with the highest CA (167°) when the grid spacing was around 60  $\mu\text{m}$ . **Figure 24** (b) shows the relationship between the contact angle and different patterns and spacing periods for the laser treatment [114].



**Figure 24:** SEM images of laser-treated surfaces: (a) Spikes, (b) LIPSS, (c) Nano-pillars [113], CA measurements at different patterns and spacing periods. (Regenerated from [114])

### 3.2 Annealing

Micro-nanostructures are important for superhydrophobicity and can be achieved with a few modifications. Annealing is a useful technique for improving the hydrophobic properties of films at elevated temperatures and in numerous conditions. Stainless steel surfaces with laser texturing can be made highly hydrophobic without needing an additional chemical coating procedure by applying a low temperature annealing post-process. When samples are aged in ambient air, the wettability shift from hydrophilicity to super-hydrophobicity takes several months, but with the suggested annealing post-process, it only takes four hours. Firstly, the samples were laser-textured using various step sizes (100, 200, 300, 400, and 500  $\mu\text{m}$ ). After laser surface texturing, the samples were annealed at low temperatures. **Figure 25** illustrates the schematic of the fabrication process of low-temperature annealing for stainless steel [48].



**Figure 25:** Fabrication process of super-hydrophobic stainless steel surface by annealing [48].

### 4. Combined Approach

In most cases, a surface modification that results in low surface energy is followed by surface roughening to provide micro-nanostructures for super-hydrophobic surfaces. While some techniques, such as laser electrodeposition and template deposition, do not require surface modification, others, such as chemical etching, the solution-immersion process, and spray coating, use coating material to modify the surface after it has been roughened [115]. The processes are mostly a combination of multiple processes that might combine various steps not covered in our discussion so far and are described in this section for fabricating super-hydrophobic surfaces on stainless steel.

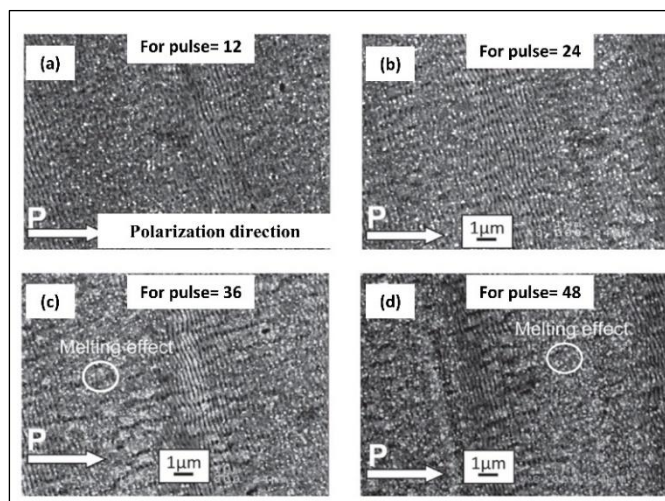


#### 4.1 Laser Processing and Coating

Exposing a work piece to a laser beam to remove material, melt it, or modify the object's surface characteristics is recognized as laser processing [116]. Laser surface texturing can enhance electrical and thermal conductivity, wettability, adhesion, and friction [117]. A coating is an application of material to a substrate with the goal of enhancing its surface properties for wear and corrosion resistance. Spin coating, Chemical vapor deposition (CVD), Plasma deposition, and electrodeposition are the most used coating processes [118]. However, combining laser ablation and coating processes can also introduce super-hydrophobicity on stainless steel.

##### 4.1.1 Laser Ablation and Chemical Vapor Deposition

While maintaining the same laser intensity, increasing pulse frequency can reduce surface roughness. Surface roughness has a substantial impact on the contact angle and promotes hydrophobicity. An experiment was conducted to determine how laser-patterned nanoscale features affected the wetting behaviour of Ti and SS sheets [119]. The samples were laser-machined utilizing 6.7 picoseconds (ps) ultraviolet laser pulses with varied pulse counts per irradiation spot. Samples were cleaned and mechanically polished before being laser machined. The studies were conducted at 6.7 ps, a fixed pulse duration. Four sets of samples with varying pulses (12 to 48), as shown in **Figure 26** were constructed to determine how the number of pulses per irradiation point affected the nanoscale structures on SS [119]. Perfluorinated octyl trichlorosilane (FOTS) was coated via chemical vapor deposition on a laser-machined surface. It was noticed that the periodicity of the ripples for the SS samples decreased as the number of pulses per irradiated site increased. In low-fluence locations, the regular ripples persist. However, these picosecond laser-induced nanoscale structures increased the metal surface's hydrophobic behaviour. In case of SS, a maximum CA of  $140^\circ \pm 3^\circ$  was achieved.

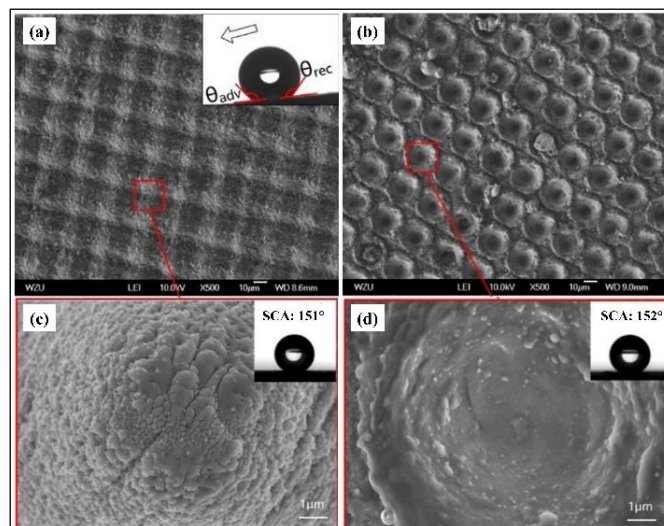


**Figure 26:** (a-d) SEM pictures of stainless-steel samples after (a) 12, (b) 24, (c) 36, and (d) 48 pulses. The indicated arrow represents the laser beam's polarization path. (Regenerated from [119])

The development of ultrashort-pulsed laser technology has transformed surface modification, making it possible to create biomimetic, superhydrophobic qualities on a massive scale. However, to lower surface energy, current research primarily uses perfluorinated and polyfluorinated alkyl compounds (PFAS), which raise serious physiological and ecological issues. A siloxane-based coating that is more environmentally friendly was created via hot-filament chemical vapor deposition [120] and effectively applied to laser-structured surfaces. Nanoscale protrusions under the uniform polymer coating formed by chemical vapor were shown to remain undamaged by the surface designs produced by femtosecond lasers. A static contact angle of  $171.6^\circ$  was attained by creating superhydrophobic surfaces by combining thin-film deposition with hierarchical surface topography. These results demonstrate the potential of combining siloxane-based CVD polymerization with laser texturing to stably customize wetting qualities.

##### 4.1.2 Laser Ablation and Spin Coating

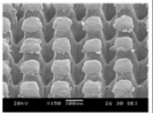
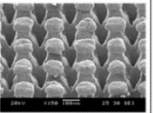
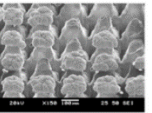



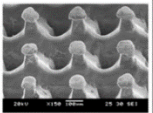
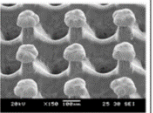
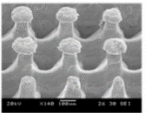



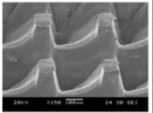
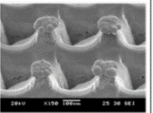
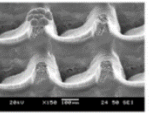



Specially prepared materials and coatings constitute the basis of anti-biofouling technology. Moreover, antifouling is a persistent objective in the maritime sector. The author [121] suggested a quick, highly controllable method for fabricating hierarchical micro/nanostructures on SS substrate. The primary objective was to make the prepared surface antifouling. Micro-groove and micro-pit arrays were designed with an optimal laser fluence of  $4 \text{ J/cm}^2$  and  $9 \text{ J/cm}^2$ , respectively. The laser-ablated specimens were chemically modified by spin-coated with silicone and heated later. The wettability test findings demonstrate that the specimens with micro-groove array and micro-pit array had CAs of  $151^\circ \pm 2^\circ$  and  $152^\circ \pm 2^\circ$ , respectively, as shown in **Figure 27** [121].



**Figure 27:** Images of laser textured specimen surface. (a)–(d) SEM images of micro-groove and micro-pit arrays [121].

#### 4.1.3 Laser Ablation and Electrodeposition

The author of the reference [122] presented a systematic approach to fabricating an extremely hydrophobic metallic surface. Successful fabrication was achieved by combining laser ablation and electrodeposition. A nanosecond pulsed laser beam was employed to fabricate the micro pillar array, and electrodeposition was utilized to build the re-entrant structure. A laser scanning path controlled the spacing of the micro pillar array. Under the experimental conditions,  $280\ \mu\text{m}$  spacing was adequate for hydrophobicity as shown in **Figure 28** [122]. At a current density of  $1280\ \mu\text{A}/\text{mm}^2$ , surface roughness was highest under the experimental conditions.

Spacing	Current Density		
	$320\ \mu\text{A}/\text{mm}^2$	$640\ \mu\text{A}/\text{mm}^2$	$1280\ \mu\text{A}/\text{mm}^2$
180 $\mu\text{m}$			
	 130°	 128°	 119°
280 $\mu\text{m}$			
	 133°	 132°	 104°
380 $\mu\text{m}$			
	 105°	 119°	 72°

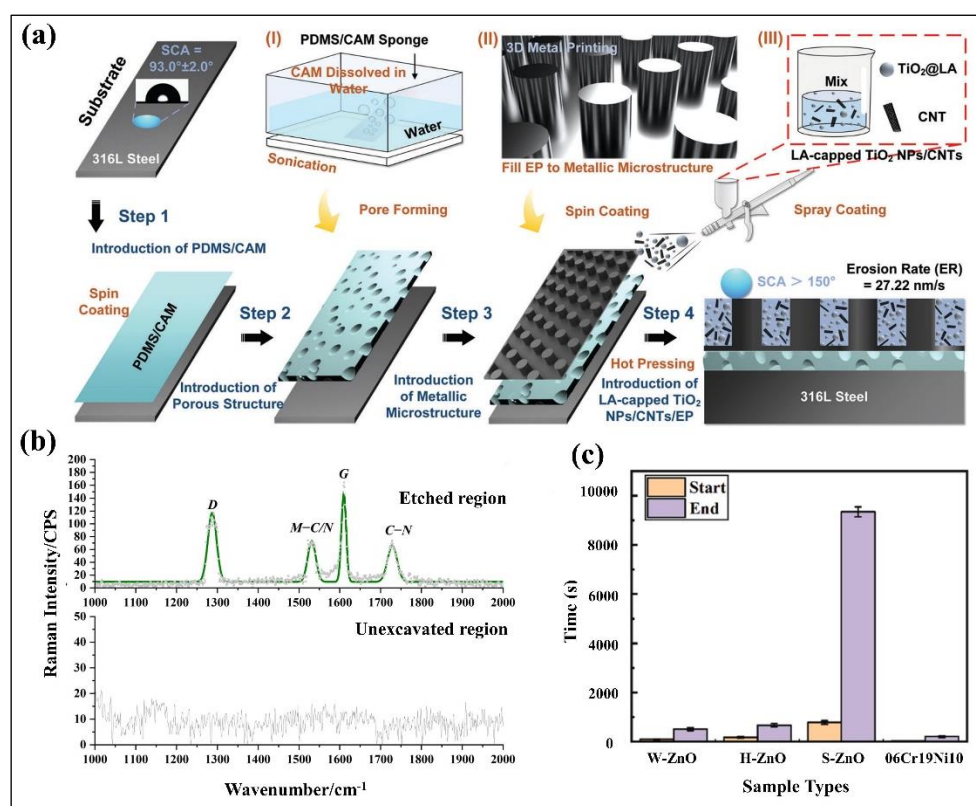
**Figure 28:** SEM image and water contact angle of micro pillar arrays fabricated using electrodeposition at the noted current densities and spacing [122].

#### 4.1.4 Miscellaneous

A biomimetic microstructure coating has been created to improve erosion and corrosion resistance in gas pipes, drawing inspiration from the surface characteristics of conch shells [123]. Metal 3D printing is used to construct the biomimetic microstructures, and a PDMS sponge containing CAM as a pore-forming agent forms the buffer layer. Through surface energy reduction and texture optimization, a superhydrophobic coating comprising CNTs, LA-modified  $\text{TiO}_2$  NPs, and epoxy resin enhances hydrophobicity. **Figure 29** (a) illustrates the stepwise fabrication process. Under harsh environmental conditions, the bionic microstructure exhibits remarkable chemical stability and resilience to corrosive agents [123].

Elastic substrate preparation is essential for dual-end supported nickel-chromium thin-film strain sensors. In the manufacturing of microelectronic components, wet etching is a crucial microfabrication technique that is frequently employed. This article [124] microprocesses the exterior dimensions and rectangular grooves of 304 stainless steel surfaces using lithography and wet etching. The ideal etching parameters were 350 g/L of  $\text{FeCl}_3$ , 150 mL/L of  $\text{HCl}$ , 100 mL/L of  $\text{HNO}_3$ , and an etching temperature of  $40^\circ\text{C}$ . As shown in **Figure 29** (b), Raman spectroscopy and XPS analyses confirmed that etching increases surface carbon content and reduces corrosion resistance. In contrast, the strain of the I-shaped substrate after wet etching is 3.5 to 4 times higher than that of the untreated rectangular substrate. Due to the extensive usage of 304 stainless steel in daily life, frost, and surface icing present serious difficulties, making research on frost inhibition essential. Conventional techniques for creating superhydrophobic surfaces are frequently expensive and complicated, which restricts their scalability.

Superhydrophobic surfaces are created on 304 stainless steel using a straightforward hydrothermal and sol-gel process in this study [125], which also assesses the icing behaviour of untreated stainless steel, hydrophobic, and superhydrophobic ZnO at low temperatures. In comparison to other surfaces, the superhydrophobic ZnO surface showed significantly improved frost retardation at ambient temperatures of  $-10^\circ\text{C}$  and  $-16^\circ\text{C}$ , delaying frost crystal propagation by about 8 minutes. **Figure 29** (c) illustrates the correlation between the icing duration and the percentage of the superhydrophobic ZnO (S-ZnO) and 304SS surfaces' coverage area. From the figure, the S-ZnO surface's ability to prevent frost is clearly visible [125].



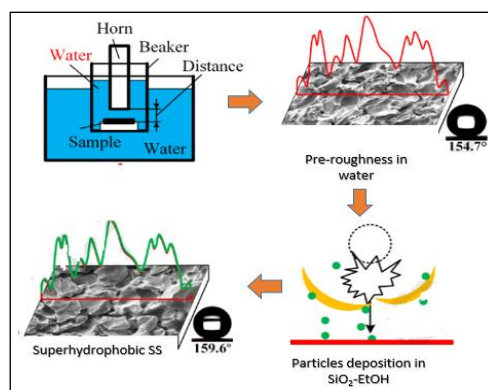
**Figure 29:** (a) Stepwise representation of the route to Biomimetic microstructure coating with a porous design (BMCP) coating [123], (b) The Raman spectroscopy of etched vs. unetched zones on 304 stainless steel [124], (c) Relationship between the time to start/end frosting time and the as-prepared samples [125].

Applications for stainless steel (SS) alloys are common in both home and industrial settings, where precise surface property control is necessary for optimizing environmental interactions. In comparison to compact SS, this study [126] presents a unique SS surface processing technique that achieves multifunctionality while retaining corrosion resistance. Through the combination of oblique-angle thin-film deposition and laser treatment of flat substrates, hierarchical SS surfaces were created. In all measured functionalities, the samples with low fluorine content outperformed SLIPS infused with fluorinated Krytox.

#### 4.2 Ultrasonic Cavitation Erosion

This experiment used cavitation erosion to generate microstructures on 304 stainless steel [127]. Microstructures were obtained employing an ultrasonic emitter. Following that, a  $\text{SiO}_2$ -EtOH solution was added to the micro structured samples. As a result, the dual micro-nanostructure was achieved. Surface modification was done using FAS-13. Consequently, an extremely hydrophobic surface was produced. **Figure 30** shows the overall fabrication process of

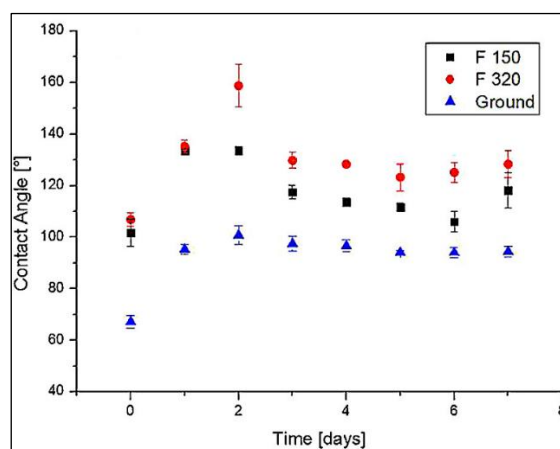
superhydrophobic surface via ultrasonic cavitation erosion [127]. The as-prepared stainless steel achieved a maximum contact angle of  $153.3^\circ$ . It was found that the cavitation erosion time depended on the sample's specific properties (hardness, phase structure).



**Figure 30:** Super-hydrophobic sample preparation process via ultrasonic cavitation erosion. (Regenerated from [127]).

#### 4.3 Sandblasting and Chemical Alternation

The current work [128] provided evidence of a straightforward, scalable process that combines chemical alteration and sandblasting to create superhydrophobic surfaces. Myristic acid was used in the chemical modification process. Further research also shows that adding chemical etching as an extra step does not seem to improve surface roughness. Sandblasted and ground surfaces were treated with an HCl and HF chemical etching solution. SiC powders of varying sizes (F150 and F320) were used for sandblasting. **Figure 31** illustrates the change of the contact angle for various samples after soaking in 0.1 M myristic acid [128]. For F320 grounded samples, the 0.1 M myristic acid solution produced the highest contact angles.

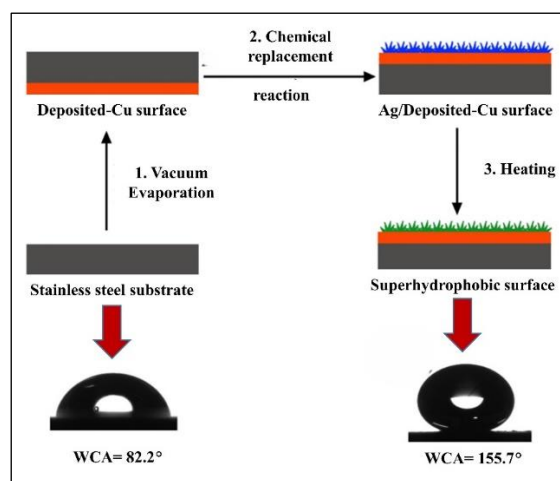


**Figure 31:** Contact angle variation of ground and sandblasted samples after soaking in 0.1 M myristic acid [128].

#### 4.4 Vacuum Evaporation, Chemical Replacement Reaction and Heating

It has been reported that super-hydrophobic surfaces on stainless steel substrates can be created via vacuum evaporation, chemical replacement reaction, and heating [129]. The substrate was first polished and thoroughly cleaned using ultrasonic. It was then covered with a Cu film created by vacuum evaporation. After that, the deposited-Cu surface was submerged in an aqueous solution of  $\text{AgNO}_3$  to initiate a chemical replacement reaction. The reaction produced a rough-structured Ag/ deposited-Cu surface. This modified surface was heated to  $100^\circ\text{C}$  and allowed to dry in the air, creating a super-hydrophobic surface. **Figure 32** schematically shows the technique of creating a superhydrophobic surface on a stainless-steel substrate, along with a WCA comparison of the treated and untreated substrates [129]. The water droplets were spherical on the superhydrophobic surface, with a WCA of about  $155.7^\circ$ .





**Figure 32:** Fabrication of super-hydrophobic surface by vacuum evaporation, chemical replacement reaction, and heating. (Regenerated from [129])

### 5. Challenges and Future Research

Each method for creating a super-hydrophobic surface works best on a specific base material. The final result may vary based on the fabrication procedure, and it is also considered a function of the base material [130]. Most researchers used 304 SS in chemical etching for fabricating SHS which is used in the cases of the combination of laser processing and chemical modification. However, 316SS is extensively used in the case of coating, electro-deposition, and laser processing. In case of laser processing, unique and expensive instruments are required. Parameters such as spacing, laser energy (fluence per pulse), and repetition rate are to be adequately set to obtain proper fabrication. Most cases require adequate knowledge and expertise for the fabrication process. In most cases, fabrication processes are developed to meet needs. Changes in the process may cause failure in expectation. Some techniques are developed for anti-icing properties, some are for anti-fouling, and some are for drag reduction. But the main target of all processes is to create an anti-corrosive, more durable, stable material in all circumstances. Solution concentration, reaction time, and temperature have a noticeable effect in the case of chemical processes over mechanical processes. A chemical reaction progresses more quickly when the temperature is raised. In the case of chemical etching, specific etching time, solution concentration, and temperature are particularly important. However, these factors are also crucial in the case of electrochemical deposition and coating. Maintaining specific solution concentrations and temperatures may create challenges in many cases. Historically, superhydrophobic coatings have been applied to material surfaces in thin layers. Simple rubbing or focused, high-pressure water streams can readily remove such coatings. Superhydrophobic surface coated with low-energy materials using various chemical methods (spin, dip, or spray coating) is unreliable. Sometimes, these methods cannot apply a superhydrophobic substance uniformly on metal surfaces. Another major issue with coating processes is the waste of reactant chemicals [131], [132]. Some processing procedures have an adverse effect on the environment. Processing time, costs, and environmental consequences must be considered for future large-scale superhydrophobic material manufacturing. Using environmentally friendly chemical reagents, fluorine-free activity, reduced energy consumption and optimization for laser processing is more practical. The creation of self-healing superhydrophobic coatings is an attractive prospect for addressing various real-world problems. It is critical to develop a superhydrophobic coating capable of regenerating low surface energy material and damaged morphology while promoting rapid healing. The challenges for fabricating a superhydrophobic surface are durability, scalability, environmental concern, cost, and self-healing. Addressing these challenges in future research would be helpful to fabricate durable superhydrophobic surface that can be scalable to industry level manufacturing.

### 6 CONCLUSIONS

In conclusion, this comprehensive review has provided an in-depth analysis of the various methodologies employed in the preparation of superhydrophobic surfaces on stainless steel substrates. Through the exploration of chemical, mechanical, and combined approaches, several key findings and insights have emerged.

Firstly, chemical techniques such as sol-gel deposition, chemical vapor deposition, and self-assembly methods have been shown to effectively induce superhydrophobicity on stainless steel surfaces. These methods offer precise control over surface chemistry and morphology, leading to robust and durable coatings with excellent water repellence properties. However, the excessive cost associated with some chemical processes, as well as potential health and environmental hazards, pose challenges that warrant consideration.

On the other hand, mechanical approaches such as laser ablation, micro/nano structuring, and sandblasting offer cost-effective alternatives for surface modification. These methods rely on physical alteration of the surface topography to achieve super-hydrophobic behaviour, often yielding hierarchical roughness structures crucial for water

repellence. Despite their simplicity and scalability, mechanical techniques may suffer from limitations in terms of coating stability and long-term durability.

Furthermore, the combination of chemical and mechanical processes has emerged as a promising strategy to overcome the limitations of individual methods while leveraging their respective advantages. By synergistically integrating chemical functionalization with mechanical roughening, enhanced superhydrophobic coatings can be achieved, offering improved stability, durability, and performance. The **Table 2** below summarizes the relevant citations with respect to related keywords.

**Table 2:** Summary of research keywords and related references on superhydrophobic stainless steel fabrication for different techniques.

	keywords	References
1	Etching	[17], [27], [42], [51], [54], [70-81], [87]
2	Coating	[43], [44], [89-101]
3	Electrochemical deposition	[45], [47], [66], [105-108]
4	Mechanical process	[48-49], [111-114]
5	Combined approaches	[115-126]
6	Ultrasonic, sandblasting, vacuum evaporation	[127-129]

## REFERENCES

- [1] T. Darmanin and F. Guittard, "Superhydrophobic and superoleophobic properties in nature," *Mater. today*, vol. 18, no. 5, pp. 273–285, 2015.
- [2] A. M. A. Mohamed, A. M. Abdullah, and N. A. Younan, "Corrosion behavior of superhydrophobic surfaces: A review," *Arab. J. Chem.*, vol. 8, no. 6, pp. 749–765, 2015, doi: 10.1016/j.arabjc.2014.03.006.
- [3] A. Lafuma and D. Quéré, "Superhydrophobic states," *Nat. Mater.*, vol. 2, no. 7, pp. 457–460, 2003.
- [4] R. S. Sutar *et al.*, "One-step candle soot-PDMS dip-coated superhydrophobic stainless steel mesh for oil-water separation," *Mater. Lett.*, vol. 357, p. 135791, 2024.
- [5] F. Li, Y. Hu, X. Feng, and G. Tian, "Preparation and Self-Cleaning Properties of a Superhydrophobic Composite Coating on a Stainless Steel Substrate," *Coatings*, vol. 14, no. 2, 2024, doi: 10.3390/coatings14020198.
- [6] X. Xue, J. Zhang, X. Sun, and B. Zhang, "Facile spraying prepared superhydrophobic coating with self-cleaning, corrosion resistance, and increased buoyancy," *Mater. Today Commun.*, vol. 40, p. 109689, 2024.
- [7] T. P. Rasitha, N. G. Krishna, B. Anandkumar, S. C. Vanithakumari, and J. Philip, "A comprehensive review on anticorrosive/antifouling superhydrophobic coatings: Fabrication, assessment, applications, challenges and future perspectives," *Adv. Colloid Interface Sci.*, p. 103090, 2024.
- [8] D. Zhang, J. Ji, C. Yan, J. Zhang, Z. An, and Y. Shen, "Research advances in bio-inspired superhydrophobic surface: Bridging nature to practical applications," *J. Ind. Eng. Chem.*, 2024.
- [9] R. Sreekumar, S. E. Thazhakkuni, and S. S. Suseelamma, "Fabrication of a robust superhydrophobic stainless steel mesh for efficient oil/water separation," *J. Ind. Eng. Chem.*, vol. 135, pp. 425–433, 2024.
- [10] J. Tan, X. Mao, W. Hu, and H. Zeng, "Facile fabrication of non-fluorine polymer brush/loop surfaces for oil/water separation and self-cleaning applications," *Sep. Purif. Technol.*, vol. 331, p. 125565, 2024.
- [11] F. O. Al-Qwairi, S. Shaheen Shah, A. H. Shabi, A. Khan, and M. A. Aziz, "Stainless Steel Mesh in Electrochemistry: Comprehensive Applications and Future Prospects," *Chem. Asian J.*, vol. 19, no. 20, p. e202400314, 2024.
- [12] T. Dhamothara Kannan, P. Sivaraj, V. Balasubramanian, T. Sonar, M. Ivanov, and S. Sathiya, "Unsymmetric rod to plate rotary friction welding of dissimilar martensitic stainless steel and low carbon steel for automotive applications—mathematical modeling and optimization," *Int. J. Interact. Des. Manuf.*, vol. 18, no. 3, pp. 1731–1759, 2024.
- [13] V. Sharma *et al.*, "Recent progress in nano-oxides and CNTs based corrosion resistant superhydrophobic coatings: A critical review," *Prog. Org. Coatings*, vol. 140, p. 105512, 2020.
- [14] "Properties of Stainless Steel & Applications - thyssenkrupp Materials (UK)." <https://www.thyssenkrupp-materials.co.uk/properties-of-stainless-steel> (accessed Nov. 16, 2022).
- [15] "Stainless Steel: Applications for Every Industry - James Duva Inc.," <https://jamesduva.com/>, Accessed: Nov. 16, 2022. [Online]. Available: <https://jamesduva.com/stainless-steel-applications-for-every-industry/>
- [16] "Does Stainless Steel Rust | Metal Casting Resources." <https://www.reliance-foundry.com/blog/does-stainless-steel-rust> (accessed Nov. 15, 2022).
- [17] L. Gao, S. Yang, H. Yang, and T. Ma, "One-Stage Method for Fabricating Superhydrophobic Stainless Steel Surface and Its Anti-Corrosion Performance," *Adv. Eng. Mater.*, vol. 19, no. 2, pp. 1–6, 2017, doi: 10.1002/adem.201600511.

- [18] O. Myronyuk, D. Baklan, and A. M. Rodin, "UV resistance of super-hydrophobic stainless steel surfaces textured by femtosecond laser pulses," in *Photonics*, MDPI, 2023, p. 1005.
- [19] M. E. Mohamed, P. S. Mekhaie, and F. M. Mahgoub, "Construction of superhydrophobic graphene-based coating on steel substrate and its ultraviolet durability and corrosion resistance properties," *Sci. Rep.*, vol. 13, no. 1, p. 590, 2023.
- [20] R. Gupta *et al.*, "A critical review on recent progress, open challenges, and applications of corrosion-resistant superhydrophobic coating," *Mater. Today Commun.*, vol. 34, p. 105201, 2023.
- [21] Y. Tang *et al.*, "Fabrication of superhydrophobic stainless steel via hybrid femtosecond laser-chemical method with wear-resistance and anti-corrosion properties," *Opt. Laser Technol.*, vol. 164, p. 109474, 2023.
- [22] X. Li *et al.*, "Waterborne robust superhydrophobic PFDTES@ TiO<sub>2</sub>-PU coating with stable corrosion resistance, long-term environmental adaptability, and delayed icing functions on Al-Li alloy," *J. Mater. Res. Technol.*, vol. 32, pp. 3357–3370, 2024.
- [23] R. Fürbacher, G. Grünsteidl, A. Otto, and G. Liedl, "Chemical and UV Durability of Hydrophobic and Icephobic Surface Layers on Femtosecond Laser Structured Stainless Steel," *Coatings*, vol. 14, no. 8, p. 924, 2024.
- [24] K. Sureshvarr *et al.*, "Control in Corrosive Behaviour of Stainless Steel (SS304) Surfaces by Enabling it as Superhydrophobic Using One-Dimensional Micro-groove Textured Surfaces," *J. Bio-and Tribo-Corrosion*, vol. 10, no. 2, p. 28, 2024.
- [25] S. Das, S. Kumar, S. K. Samal, S. Mohanty, and S. K. Nayak, "A review on superhydrophobic polymer nanocoatings: recent development and applications," *Ind. Eng. Chem. Res.*, vol. 57, no. 8, pp. 2727–2745, 2018.
- [26] M. A. Jafar Mazumder, "Global Impact of Corrosion: Occurrence, Cost and Mitigation," *Glob. J. Eng. Sci.*, vol. 5, no. 4, pp. 0–4, 2020, doi: 10.33552/gjes.2020.05.000618.
- [27] H. Zhang, Y. Tuo, Q. Wang, B. Jin, and L. Yin, "Fabrication and drag reduction of superhydrophobic surface on steel substrates," *Surf. Eng.*, vol. 0, no. 0, pp. 1–7, 2017, doi: 10.1080/02670844.2017.1317423.
- [28] E. Khalili and M. Sarafbidabad, "Combination of laser patterning and nano PTFE sputtering for the creation a super-hydrophobic surface on 304 stainless steel in medical applications," *Surfaces and Interfaces*, vol. 8, pp. 219–224, 2017.
- [29] S. Zouaghi *et al.*, "Antifouling biomimetic liquid-infused stainless steel: application to dairy industrial processing," *ACS Appl. Mater. Interfaces*, vol. 9, no. 31, pp. 26565–26573, 2017.
- [30] K. Sukhareva, V. Chernetsov, and I. Burmistrov, "A review of antimicrobial polymer coatings on steel for the food processing industry," *Polymers (Basel)*, vol. 16, no. 6, p. 809, 2024.
- [31] A. Abolins, "Laser radiation made hydrophobic surface on stainless steel for food industry, a review," in *ENVIRONMENT. TECHNOLOGIES. RESOURCES. Proceedings of the International Scientific and Practical Conference*, 2024, pp. 358–362.
- [32] M. M. DEWIDAR, K. A. KHALIL, and J. K. LIM, "Processing and mechanical properties of porous 316L stainless steel for biomedical applications," *Trans. Nonferrous Met. Soc. China (English Ed.)*, vol. 17, no. 3, 2007, doi: 10.1016/S1003-6326(07)60117-4.
- [33] C. Hu, S. Liu, B. Li, H. Yang, C. Fan, and W. Cui, "Micro-/nanometer rough structure of a superhydrophobic biodegradable coating by electrospraying for initial anti-bioadhesion," *Adv. Healthc. Mater.*, vol. 2, no. 10, pp. 1314–1321, 2013.
- [34] L. Mishchenko, B. Hatton, V. Bahadur, J. A. Taylor, T. Krupenkin, and J. Aizenberg, "Design of ice-free nanostructured surfaces based on repulsion of impacting water droplets," *ACS Nano*, vol. 4, no. 12, pp. 7699–7707, 2010.
- [35] A. Ganne, K. I. Maslakov, and A. I. Gavrilov, "Anti-icing properties of superhydrophobic stainless steel mesh at subzero temperatures," *Surf. Innov.*, vol. 5, no. 3, pp. 154–160, 2017.
- [36] Y. Bai, H. Zhang, Y. Shao, H. Zhang, and J. Zhu, "Recent progresses of superhydrophobic coatings in different application fields: An overview," *Coatings*, vol. 11, no. 2, p. 116, 2021.
- [37] X. Chen *et al.*, "Construction of superhydrophobic surfaces with different water adhesion on the low-temperature steels by picosecond laser processing," *Surf. Coatings Technol.*, vol. 477, p. 130340, 2024.
- [38] H. Wang, P. Cao, S. Xu, G. Cui, Z. Chen, and Q. Yin, "Anti-icing performance of hydrophobic coatings on stainless steel surfaces," *Heliyon*, 2024.
- [39] J. Fu, X. Liao, Y. Ji, Y. Mo, and J. Zhang, "Research Progress on Preparation of Superhydrophobic Surface and Its Application in the Field of Marine Engineering," *J. Mar. Sci. Eng.*, vol. 12, no. 10, p. 1741, 2024.
- [40] P. Zhang *et al.*, "Constructing carbon nanotube (CNTs)/silica superhydrophobic coating with multi-stage rough structure for long-term anti-corrosion and low-temperature anti-icing in the marine environment," *Compos. Sci. Technol.*, vol. 257, p. 110798, 2024.
- [41] "What are superhydrophobic surfaces?" <https://www.biolinscientific.com/blog/what-are-superhydrophobic-surfaces> (accessed Nov. 15, 2022).
- [42] Y. Liu, Y. Bai, J. Jin, L. Tian, Z. Han, and L. Ren, "Facile fabrication of biomimetic superhydrophobic surface with anti-frosting on stainless steel substrate," *Appl. Surf. Sci.*, vol. 355, pp. 1238–1244, 2015, doi: 10.1016/j.apsusc.2015.08.027.

- [43] Y. Hu, H. He, and Y. Ma, "Preparation of superhydrophobic SiO<sub>2</sub> coating on stainless steel substrate," *Key Eng. Mater.*, vol. 512–515, pp. 1028–1031, 2012, doi: 10.4028/www.scientific.net/KEM.512-515.1028.
- [44] T. T. Isimjan, T. Wang, and S. Rohani, "A novel method to prepare superhydrophobic, UV resistance and anti-corrosion steel surface," *Chem. Eng. J.*, vol. 210, pp. 182–187, 2012, doi: 10.1016/j.cej.2012.08.090.
- [45] J. Liang, D. Li, D. Wang, K. Liu, and L. Chen, "Preparation of stable superhydrophobic film on stainless steel substrate by a combined approach using electrodeposition and fluorinated modification," *Appl. Surf. Sci.*, vol. 293, pp. 265–270, 2014, doi: 10.1016/j.apsusc.2013.12.147.
- [46] K. Sun *et al.*, "Anti-biofouling superhydrophobic surface fabricated by picosecond laser texturing of stainless steel," *Appl. Surf. Sci.*, vol. 436, pp. 263–267, 2018, doi: 10.1016/j.apsusc.2017.12.012.
- [47] Z. Xu, D. Jiang, Z. Wei, J. Chen, and J. Jing, "Fabrication of superhydrophobic nano-aluminum films on stainless steel meshes by electrophoretic deposition for oil-water separation," *Appl. Surf. Sci.*, vol. 427, pp. 253–261, 2018, doi: 10.1016/j.apsusc.2017.08.189.
- [48] C. V. Ngo and D. M. Chun, "Fast wettability transition from hydrophilic to superhydrophobic laser-textured stainless steel surfaces under low-temperature annealing," *Appl. Surf. Sci.*, vol. 409, pp. 232–240, 2017, doi: 10.1016/j.apsusc.2017.03.038.
- [49] L. Gemini, M. Faucon, L. Romoli, and R. Kling, "High throughput laser texturing of super-hydrophobic surfaces on steel," *Laser-based Micro- Nanoprocessing XI*, vol. 10092, p. 100921G, 2017, doi: 10.1117/12.2252649.
- [50] "Chemical Process Definition | Law Insider." <https://www.lawinsider.com/dictionary/chemical-process> (accessed Nov. 10, 2022).
- [51] J. H. Kim, A. Mirzaei, H. W. Kim, and S. S. Kim, "Facile fabrication of superhydrophobic surfaces from austenitic stainless steel (AISI 304) by chemical etching," *Appl. Surf. Sci.*, vol. 439, no. Aisi 304, pp. 598–604, 2018, doi: 10.1016/j.apsusc.2017.12.211.
- [52] Z. Zhang *et al.*, "Ultrasonic assisted rapid preparation of superhydrophobic stainless steel surface and its application in oil/water separation," *Ultrason. Sonochem.*, vol. 81, p. 105848, 2021.
- [53] C. Lee, J. M. Kim, and H. Kim, "A study on Water-Proof Characteristics of a Stainless Steel Mesh by Electrochemical Etching Process," *Tribol. Lubr.*, vol. 37, no. 5, pp. 189–194, 2021.
- [54] Y. Zhang, Z. Zhang, J. Yang, Y. Yue, and H. Zhang, "Fabrication of superhydrophobic surface on stainless steel by two-step chemical etching," *Chem. Phys. Lett.*, vol. 797, p. 139567, 2022.
- [55] H. Hu, X. Hong, and Y. Gao, "The construction of superhydrophobic structure on stainless steel by an optimized chemical etching technics," *J. Eng. Mater. Technol.*, vol. 144, no. 2, p. 21001, 2022.
- [56] M. Wysard Jr, R. Vasconcelos, E. A. de Souza, M. Costa, and S. S. Camargo Jr, "Very simple method to produce superhydrophobic stainless steel surfaces at room temperature," *Mater. Chem. Phys.*, vol. 307, p. 128203, 2023.
- [57] S. Zhu, W. Deng, and Y. Su, "Recent advances in preparation of metallic superhydrophobic surface by chemical etching and its applications," *Chinese J. Chem. Eng.*, vol. 61, pp. 221–236, 2023.
- [58] F. De Nicola, P. Castrucci, M. Scarselli, F. Nanni, I. Cacciotti, and M. De Crescenzi, "Super-hydrophobic multi-walled carbon nanotube coatings for stainless steel," *Nanotechnology*, vol. 26, no. 14, p. 145701, 2015, doi: 10.1088/0957-4484/26/14/145701.
- [59] Y. Jiang, C. Liu, Y. Li, and A. Huang, "Stainless-steel-net-supported superhydrophobic COF coating for oil/water separation," *J. Memb. Sci.*, vol. 587, p. 117177, 2019.
- [60] S. M. Gateman *et al.*, "Corrosion of one-step superhydrophobic stainless-steel thermal spray coatings," *ACS Appl. Mater. Interfaces*, vol. 12, no. 1, pp. 1523–1532, 2019.
- [61] R. S. Sutar *et al.*, "A facile approach for oil-water separation using superhydrophobic polystyrene-silica coated stainless steel mesh bucket," *Mar. Pollut. Bull.*, vol. 198, p. 115790, 2024.
- [62] X. Zhang *et al.*, "Preparation of robust superhydrophobic stainless steel mesh for Oil-Water separation through Mn-Assisted control of one-step electrodeposited Zn growth," *Chem. Eng. J.*, vol. 498, p. 155369, 2024.
- [63] X. Wang, B.-B. Wang, B. Deng, and Z.-M. Xu, "Superior droplet bouncing, anti-icing/anti-frosting and self-cleaning performance of an outstanding superhydrophobic PTFE coating," *Cold Reg. Sci. Technol.*, p. 104229, 2024.
- [64] V. K. Mishra and R. S. Raman, "Effect of PH on the development of superhydrophobic coating on stainless steel," *Int. J. Mater. Eng. Innov.*, vol. 15, no. 2, pp. 143–156, 2024.
- [65] C. Fan *et al.*, "Fabrication and Properties of Superhydrophobic Colored Stainless Steel Surface for Decoration and Anti-Corrosion," *Coatings*, vol. 14, no. 9, p. 1117, 2024.
- [66] S. Li, Y. Liu, Z. Tian, X. Liu, Z. Han, and L. Ren, "Biomimetic superhydrophobic and antibacterial stainless-steel mesh via double-potentiostatic electrodeposition and modification," *Surf. Coatings Technol.*, vol. 403, no. May, p. 126355, 2020, doi: 10.1016/j.surfcoat.2020.126355.
- [67] J. Xu *et al.*, "Fabrication of superhydrophobic stainless-steel mesh for oil-water separation by jet electrodeposition," *Colloids Surfaces A Physicochem. Eng. Asp.*, vol. 649, p. 129434, 2022.
- [68] V. Athulya, S. C. Vanithakumari, A. R. Shankar, and S. Ningshen, "Electrodeposition of myristate based superhydrophobic coatings on steel with enhanced corrosion resistance and self-cleaning property," *Surf.*



- Coatings Technol.*, vol. 489, p. 131114, 2024.
- [69] W. Zhang *et al.*, "A rapid two-step process to prepare a high-throughput, efficient, reusable superhydrophobic-superoleophilic stainless steel mesh for oil/water separation," *J. Adhes. Sci. Technol.*, pp. 1–27, 2024.
- [70] A. Kumar and D. Nanda, *Methods and fabrication techniques of superhydrophobic surfaces*. Elsevier Inc., 2019. doi: 10.1016/B978-0-12-816671-0.00004-7.
- [71] A. Bahgat Radwan, A. M. Abdullah, and N. A. Alnuaimi, "Recent advances in corrosion resistant superhydrophobic coatings," *Corros. Rev.*, vol. 36, no. 2, pp. 127–153, 2018, doi: 10.1515/correv-2017-0012.
- [72] T. Rezayi and M. H. Entezari, "Toward a durable superhydrophobic aluminum surface by etching and ZnO nanoparticle deposition," *J. Colloid Interface Sci.*, vol. 463, pp. 37–45, 2016, doi: 10.1016/j.jcis.2015.10.029.
- [73] H.-J. Choi, J.-H. Shin, S. Choo, S.-W. Ryu, Y.-D. Kim, and H. Lee, "Fabrication of superhydrophobic and oleophobic Al surfaces by chemical etching and surface fluorination," *Thin Solid Films*, vol. 585, pp. 76–80, 2015.
- [74] Y. Chen, Z. Guo, J. Xu, L. Shi, J. Li, and Y. Zhang, "Inspired superhydrophobic surfaces by a double-metal-assisted chemical etching route," *Mater. Res. Bull.*, vol. 47, no. 7, pp. 1687–1692, 2012, doi: 10.1016/j.materresbull.2012.03.049.
- [75] C. Zhilei, S. Maobing, and W. Lida, "Cathodic etching for fabrication of super-hydrophobic aluminum coating with micro/nano-hierarchical structure," *J. Solid State Electrochem.*, vol. 17, no. 10, pp. 2661–2669, 2013, doi: 10.1007/s10008-013-2141-0.
- [76] Z. Zhang *et al.*, "Preparation of intricate nanostructures on 304 stainless steel surface by SiO<sub>2</sub>-assisted HF etching for high superhydrophobicity," *Colloids Surfaces A Physicochem. Eng. Asp.*, vol. 586, p. 124287, 2020.
- [77] H. F. Zhang, X. W. Liu, M. Zhao, D. Wang, and C. Z. Shi, "Fabrication of super-hydrophobic surface on stainless steel using chemical etching method," *Key Eng. Mater.*, vol. 562–565, pp. 33–38, 2013, doi: 10.4028/www.scientific.net/KEM.562-565.33.
- [78] "Anti-Corrosion Protective Coatings for Steel - PFI Inc." <https://www.pfiinc.com/anti-corrosion-protective-coatings-for-steel/> (accessed Nov. 11, 2022).
- [79] C.-J. Weng *et al.*, "Advanced anticorrosive coatings prepared from the mimicked xanthosoma sagittifolium-leaf-like electroactive epoxy with synergistic effects of superhydrophobicity and redox catalytic capability," *Chem. Mater.*, vol. 23, no. 8, pp. 2075–2083, 2011.
- [80] J.-D. Brassard, D. K. Sarkar, J. Perron, A. Audibert-Hayet, and D. Melot, "Nano-micro structured superhydrophobic zinc coating on steel for prevention of corrosion and ice adhesion," *J. Colloid Interface Sci.*, vol. 447, pp. 240–247, 2015.
- [81] Y. Chen, W. Deng, S. Zhu, G. Chen, L. Wang, and Y. Su, "Preparation of super-hydrophobic surface with micro-nano layered structure on 316 stainless steel by one-step wet chemical method," *Colloids Surfaces A Physicochem. Eng. Asp.*, vol. 655, no. September, p. 130291, 2022, doi: 10.1016/j.colsurfa.2022.130291.
- [82] J. S. Jayan, D. Jayadev, Z. S. Pillai, K. Joseph, and A. Saritha, "The stability of the superhydrophobic surfaces," in *Superhydrophobic Polymer Coatings*, Elsevier, 2019, pp. 123–159.
- [83] G. Liu, Y. Yuan, Z. Jiang, J. Youdong, and W. Liang, "Anti-frosting/anti-icing property of nano-ZnO superhydrophobic surface on Al alloy prepared by radio frequency magnetron sputtering," *Mater. Res. Express*, vol. 7, no. 2, 2020, doi: 10.1088/2053-1591/ab6e33.
- [84] J. U. Jeong, J. P. Chakrapani Gunarasan, and J. W. Lee, "Facile fabrication of microstructured superhydrophilic and superhydrophobic STS316L," *Curr. Appl. Phys.*, vol. 65, no. April, pp. 60–67, 2024, doi: 10.1016/j.cap.2024.06.006.
- [85] Z. Zhao, H. Chen, X. Liu, H. Liu, and D. Zhang, "Development of high-efficient synthetic electric heating coating for anti-icing/de-icing," *Surf. Coatings Technol.*, vol. 349, pp. 340–346, Sep. 2018, doi: 10.1016/J.SURFCOAT.2018.06.011.
- [86] S. Jung, M. Dorrestijn, D. Raps, A. Das, C. M. Megaridis, and D. Poulikakos, "Are superhydrophobic surfaces best for icephobicity?," *Langmuir*, vol. 27, no. 6, pp. 3059–3066, 2011.
- [87] N. Wang, D. Xiong, M. Li, Y. Deng, Y. Shi, and K. Wang, "Ac ce pt cr t," *Appl. Surf. Sci.*, 2015, doi: 10.1016/j.apsusc.2015.06.203.
- [88] G. A. Howarth and H. L. Manock, "Water-borne polyurethane dispersions and their use in functional coatings," *Surf. coatings Int.*, vol. 80, no. 7, pp. 324–328, 1997.
- [89] "Coating Meaning | What is Coating Definition | Labelplanet." <https://www.labelplanet.co.uk/glossary/coating/> (accessed Dec. 15, 2023).
- [90] G. A. Howarth, "The synthesis of a legislation compliant corrosion protection paint system, based on waterborne epoxy, urethane and oxazolidine technology." MSc Thesis, April, Imperial College London, 1997.
- [91] A. O. Ijaola, P. K. Farayibi, and E. Asmatulu, "Superhydrophobic coatings for steel pipeline protection in oil and gas industries: A comprehensive review," *J. Nat. Gas Sci. Eng.*, vol. 83, p. 103544, 2020.
- [92] M. Mozammel, M. Khajeh, and N. N. Ilkhechi, "Effect of Surface Roughness of 316 L Stainless Steel Substrate on the Morphological and Super-Hydrophobic Property of TiO<sub>2</sub> Thin Films Coatings," *Silicon*, vol. 10, no.

- 6, pp. 2603–2607, 2018, doi: 10.1007/s12633-018-9796-1.
- [93] A. N. Majeed, R. S. Sabry, and M. A. Abid, "Fabrication of Superhydrophobic (TiO<sub>2</sub> /PDMS) Coating For Oil-Water Separation," *IOP Conf. Ser. Earth Environ. Sci.*, vol. 1325, no. 1, 2024, doi: 10.1088/1755-1315/1325/1/012003.
- [94] X. Zhang, X. Liu, J. Laakso, E. Levänen, and T. Mäntylä, "Easy-to-clean property and durability of superhydrophobic flaky  $\gamma$ -alumina coating on stainless steel in field test at a paper machine," *Appl. Surf. Sci.*, vol. 258, no. 7, pp. 3102–3108, 2012, doi: 10.1016/j.apsusc.2011.11.045.
- [95] J. Li, H. Wan, Y. Ye, H. Zhou, and J. Chen, "One-step process for the fabrication of superhydrophobic surfaces with easy reparability," *Appl. Surf. Sci.*, vol. 258, no. 7, pp. 3115–3118, 2012, doi: 10.1016/j.apsusc.2011.11.047.
- [96] "Atmospheric Water Generation Research | US EPA." <https://www.epa.gov/water-research/atmospheric-water-generation-research> (accessed Jun. 27, 2023).
- [97] F. Zohra, M. Akanda, and B. Asiabanpour, "The Effect of Macroscopic and Microscopic Patterns of Stainless Steel Surface on the Efficiency of Dropwise Condensation and Precipitation," *Int. J. Eng. Mater. Manuf.*, vol. 6, no. 3, pp. 163–169, 2021, doi: 10.26776/ijemm.06.03.2021.07.
- [98] X. Chen, Y. Gong, D. Li, and H. Li, "Robust and easy-repairable superhydrophobic surfaces with multiple length-scale topography constructed by thermal spray route," *Colloids Surfaces A Physicochem. Eng. Asp.*, vol. 492, pp. 19–25, 2016, doi: 10.1016/j.colsurfa.2015.12.017.
- [99] C. Fan *et al.*, "Fabrication and Properties of Superhydrophobic Colored Stainless Steel Surface for Decoration and Anti-Corrosion," *Coatings*, vol. 14, no. 9, p. 1117, 2024, doi: 10.3390/coatings14091117.
- [100] C. Chen, D. Weng, S. Chen, A. Mahmood, and J. Wang, "Development of Durable, Fluorine-free, and Transparent Superhydrophobic Surfaces for Oil/Water Separation," *ACS Omega*, vol. 4, no. 4, pp. 6947–6954, 2019, doi: 10.1021/acsomega.9b00518.
- [101] J. Zhou *et al.*, "Experimental study on impact icing of the superhydrophobic surfaces with cruciferous bionic structure," *AIP Adv.*, vol. 14, no. 5, 2024, doi: 10.1063/5.0210256.
- [102] "What is an Electrochemical Deposition? - Definition from Corrosionpedia." <https://www.corrosionpedia.com/definition/5493/electrochemical-deposition> (accessed Nov. 12, 2022).
- [103] M. W. Losey, J. J. Kelly, N. D. Badgayan, S. K. Sahu, and P. S. B. T.-R. M. in M. S. and M. E. Rama Sreekanth, "Electrodeposition," Elsevier, 2017. doi: <https://doi.org/10.1016/B978-0-12-803581-8.10137-7>.
- [104] B. Mundotiya and W. Ullah, "Morphology Controlled Synthesis of the Nanostructured Gold by Electrodeposition Techniques," 2018. doi: 10.5772/intechopen.80846.
- [105] Y. Fan, Y. He, P. Luo, X. Chen, and B. Liu, "A facile electrodeposition process to fabricate corrosion-resistant superhydrophobic surface on carbon steel," *Appl. Surf. Sci.*, vol. 368, pp. 435–442, 2016, doi: 10.1016/j.apsusc.2016.01.252.
- [106] A. M. Escobar, N. Llorca-Isern, and O. Rius-Ayra, "Identification of the mechanism that confers superhydrophobicity on 316L stainless steel," *Mater. Charact.*, vol. 111, pp. 162–169, 2016, doi: 10.1016/j.matchar.2015.11.026.
- [107] X. Zhang *et al.*, "An ultra-thin nickel electrodeposited stainless steel mesh with superhydrophobic property and high mechanical durability for oil-water separation," *J. Environ. Chem. Eng.*, vol. 12, no. 1, p. 111692, 2024, doi: 10.1016/j.jece.2023.111692.
- [108] M. Fatahiamirdehi, M. Mahani, S. F. Mirseyed, A. Rostamian, and M. Ostadhassan, "Enhancing corrosion resistance of 316L stainless steel through electrochemical deposition of polyaniline coatings in acidic environments," *J. Mater. Sci.*, vol. 59, no. 31, pp. 14716–14727, 2024, doi: 10.1007/s10853-024-10047-2.
- [109] "Mechanical processing Definition | Law Insider." <https://www.lawinsider.com/dictionary/mechanical-processing> (accessed Jan. 10, 2025).
- [110] "What is Laser Texturing and How it Works." <https://www.laserax.com/laser-texturing> (accessed Jun. 27, 2023).
- [111] H. Kenar *et al.*, "Femtosecond laser treatment of 316L improves its surface nanoroughness and carbon content and promotes osseointegration: An in vitro evaluation," *Colloids Surfaces B Biointerfaces*, vol. 108, pp. 305–312, 2013, doi: 10.1016/j.colsurfb.2013.02.039.
- [112] H. Kenar *et al.*, "Femtosecond laser treatment of 316L improves its surface nanoroughness and carbon content and promotes osseointegration: An in vitro evaluation," *Colloids Surfaces B Biointerfaces*, vol. 108, pp. 305–312, 2013.
- [113] A. H. A. Lutey *et al.*, "Towards laser-textured antibacterial surfaces," *Sci. Rep.*, vol. 8, no. 1, pp. 1–11, 2018, doi: 10.1038/s41598-018-28454-2.
- [114] G. Lim and M. B. G. Jun, "Ac ce p te d us ip t," *Appl. Surf. Sci.*, 2014, doi: 10.1016/j.apsusc.2014.05.224.
- [115] H. M. Ali, M. A. Qasim, S. Malik, and G. Murtaza, "Techniques for the fabrication of super-hydrophobic surfaces and their heat transfer applications," *Heat Transf. Model. Methods Appl*, vol. 1, pp. 283–315, 2018.
- [116] "Laser Processing Technology (Application & Development) | MachineMfg." <https://www.machinemfg.com/laser-processing-technology/> (accessed Dec. 22, 2022).
- [117] "What is Laser Texturing and How it Works." <https://www.laserax.com/laser-texturing> (accessed Nov. 26, 2022).

- [118] "What is a coating? - TWI." <https://www.twi-global.com/technical-knowledge/faqs/faq-what-is-a-coating> (accessed Dec. 22, 2022).
- [119] R. Jagdheesh, B. Pathiraj, E. Karatay, and A. J. Huis, "Laser-Induced Nanoscale Superhydrophobic Structures on Metal Surfaces," pp. 8464–8469, 2011.
- [120] G. Schnell, J. Piehl, T. Hartig, N. Dubhorn, and A. Aliyeva, "PFAS-free Superhydrophobic Surfaces using Femtosecond Laser Processing and Hot-Filament Chemical Vapor Deposition," pp. 1–18.
- [121] K. Sun *et al.*, "Anti-biofouling superhydrophobic surface fabricated by picosecond laser texturing of stainless steel," *Appl. Surf. Sci.*, vol. 436, no. 51135005, pp. 263–267, 2018, doi: 10.1016/j.apsusc.2017.12.012.
- [122] M. H. Kwon, H. S. Shin, and C. N. Chu, "Fabrication of a super-hydrophobic surface on metal using laser ablation and electrodeposition," *Appl. Surf. Sci.*, vol. 288, pp. 222–228, 2014, doi: 10.1016/j.apsusc.2013.10.011.
- [123] X. Zang *et al.*, "A Robust Biomimetic Superhydrophobic Coating with Superior Mechanical Durability and Chemical Stability for Inner Pipeline Protection," *Adv. Sci.*, vol. 11, no. 12, pp. 1–9, 2024, doi: 10.1002/advs.202305839.
- [124] D. Song and W. Wu, "Study on Electrical and Mechanical Properties of Double-End Supported Elastic Substrate Prepared by Wet Etching Process," *Micromachines*, vol. 15, no. 7, 2024, doi: 10.3390/mi15070929.
- [125] Y. Deng *et al.*, "Delaying frost formation by controlling surface chemistry of ZnO-coated 304 stainless steel surfaces," *Colloids Surfaces A Physicochem. Eng. Asp.*, vol. 696, no. May, p. 134375, 2024, doi: 10.1016/j.colsurfa.2024.134375.
- [126] L. Montes *et al.*, "Long-lasting low fluorinated stainless steel hierarchical surfaces for omniphobic, anti-fouling and anti-icing applications," *Surfaces and Interfaces*, vol. 46, no. February, 2024, doi: 10.1016/j.surfin.2024.104167.
- [127] F. Chen, J. Du, and S. Huang, "Fabrication of repairable anti-corrosive superhydrophobic surfaces with micro-nano structures by ultrasonic cavitation," *Appl. Surf. Sci.*, vol. 541, p. 148605, 2021, doi: 10.1016/j.apsusc.2020.148605.
- [128] M. Alonso Frank, A. R. Boccaccini, and S. Virtanen, "A facile and scalable method to produce superhydrophobic stainless steel surface," *Appl. Surf. Sci.*, vol. 311, pp. 753–757, 2014, doi: 10.1016/j.apsusc.2014.05.152.
- [129] N. Wang, Q. Wang, S. Xu, and X. Zheng, "Eco-Friendly and Safe Method of Fabricating Superhydrophobic Surfaces on Stainless Steel Substrates," *J. Phys. Chem. C*, vol. 123, no. 42, pp. 25738–25746, 2019, doi: 10.1021/acs.jpcc.9b07641.
- [130] K. Manoharan and S. Bhattacharya, "Superhydrophobic surfaces review: Functional application, fabrication techniques and limitations," *J. Micromanufacturing*, vol. 2, no. 1, pp. 59–78, 2019, doi: 10.1177/2516598419836345.
- [131] E. K. Hussmann, "Dip coatings: characteristics, properties, applications," in *Optical Surface Technology*, SPIE, 1983, pp. 152–159.
- [132] K. Seiders, B. Yake, and W. Olympia, "Washington State Toxics Monitoring Program: Exploratory Monitoring of Toxic Contaminants in Edible Fish Tissue and Freshwater Environments," *Draft Rep. dated*, vol. 30, 2002.

Declaration: The authors of this article declare that all Figures are appropriately referenced and used under "Fair use policy under the U.S. copyright statute" <https://www.copyright.gov/fair-use/>